*IN -46*

# A Laboratory Study on the Phase Transition for Polar Stratospheric Cloud Particles

Edward H. Teets, Jr.

# A Laboratory Study on the Phase Transition for Polar Stratospheric Cloud Particles

Edward H. Teets, Jr.
*University of Reno*
*Reno, Nevada*

National Aeronautics and
Space Administration

Dryden Flight Research Center
Edwards, California 93523-0273

# CONTENTS

# TABLES

# FIGURES

# ACKNOWLEDGMENTS

I would like to thank Dr. John Hallett for being a terrific advisor with the insight and knowledge to lead me through the completion of this thesis. Also, I would like to thank Dr. Alan Gertler and Dr. John Frederick for their willingness to serve on my committee and help me when I had questions.

I would also like to thank Bill McCain of PRC Inc. and L. J. Ehrenberger of NASA Dryden Flight Research Center for giving me encouragement, and work experience while continuing my education.

To my parents, Edward and Lynn Teets, for their unconditional support and encouragement through my school and life. Without these two great people this thesis would not be possible.

Last but not least, I would like to thank my wife Elisa Olson Teets for her patience and support during my graduate study.

# ABSTRACT

The nucleation and growth of different phases of simulated polar stratospheric cloud (PSC) particles were investigated in the laboratory. Solutions and mixtures of solutions at concentrations 1 to 5 $m$ (molality) of ammonium sulfate, ammonium bisulfate, sodium chloride, sulfuric acid, and nitric acid were supercooled to prescribed temperatures below their equilibrium melting point. These solutions were contained in small diameter glass tubing of volumes ranging from 2.6 to 0.04 ml. Samples were nucleated by insertion of an ice crystal, or in some cases by a liquid nitrogen cooled wire. Crystallization velocities were determined by timing the crystal growth front passages along the glass tubing. Solution mixtures containing aircraft exhaust (soot) were also examined. Crystallization rates increased as $\Delta T^2$, where $\Delta T$ is the supercooling for weak solutions (2 $m$ or less). The higher concentrated solutions (>3 $m$) showed rates significantly less than $\Delta T^2$. This reduced rate suggested an onset of a glass phase. Results were applied to the nucleation of highly concentrated solutions at various stages of polar stratospheric cloud development within the polar stratosphere.

# NOMENCLATURE

| | |
|---|---|
| $A$ | constant for a given substance |
| $a$ | a function of the environment variable, $2\sigma/\rho_L R_v T$ |
| AAOE | Airborne Antarctic Ozone Experiment |
| ACS | American Chemical Society |
| $b$ | variable, $3im_v/4\pi\rho_L m_s$ |
| CCN | condensation cloud nuclei |
| CFC | chlorofluorocarbons |
| $D$ | diameter |
| DFRC | NASA Dryden Flight Research Center, Edwards, California |
| $e$ | inverse of natural log, 2.71828 |
| $e'$ | vapor pressure over the solution |
| $e_s$ | vapor pressure of the pure solution |
| $hv$ | solar energy, nm |
| JPL | Jet Propulsion Laboratory |
| $K_f$ | freezing point depression constant |
| M | mass |
| $m$ | moles of solute per kilogram of solvent |
| $m_s$ | mass of solute, K |
| n | moles of solute |
| $N_0$ | number of effective solute molecules of mass |
| $n_0$ | moles of solvent |
| NAT | nitric acid trihydrate |
| NMR | number mixing ratios |
| OCS | carbonyl sulfide |
| P | best fit slope of the growth velocity on a log-log plot |
| PSC | polar stratospheric cloud |

| | |
|---|---|
| $r$ | radius |
| $R_v$ | universal gas constant |
| RH | relative humidity |
| SAM II | Stratospheric Aerosol Measurement II |
| SAT | sulfuric acid tetrahydrate |
| $T$ | temperature |
| $V_r$ | growth velocity, cm sec$^{-1}$ |
| $\Delta G$ | Gibbs free energy |
| $\Delta T$ | degree of supercooling for weak solutions |
| $\Delta T_f$ | temperature freezing point depression |
| $\eta$ | viscosity |
| $\kappa$ | thermal diffusivity of glass or liquid, cm$^2$ sec$^{-1}$ |
| $\rho_L$ | density of the liquid |
| $\sigma$ | surface tension |
| $\tau$ | thermal equilibrium |

# CHAPTER 1: INTRODUCTION

Nucleation and growth of polar stratospheric cloud (PSC) particles has become of great interest because of the recent discovery of the PSC link to ozone destruction. PSCs form in the polar vortices, on $H_2SO_4$-$nH_2O$ nuclei particles. This process occurs by the deliquescence of nitric acid ($HNO_3$) and water ($H_2O$) onto these particles as the temperatures in the stratosphere drop during the Arctic or Antarctic winters. A knowledge of the stratospheric aerosol nucleation process and how these particles grow is an important aspect in understanding the formation of these clouds. In general, the nucleation process is dominated by the presence of impurity nucleation, which prevents the occurrence of substantial supercooling. However, on occasion nucleation can be initiated in the absence of impurities by growth from large clusters of atoms and molecules. This is homogeneous nucleation of the substance by itself, as opposed to heterogeneous nucleation by impurity.

In the laboratory experimental techniques for the study of nucleation processes follow the simple method of taking smaller and smaller samples until the probability of having impurity-induced heterogeneous nucleation is reduced to insignificant levels. Nature applies this technique very effectively in clouds in the atmosphere, which contain liquid water or solution droplets less than about 10 $\mu$m in diameter. Studies have shown these droplets can be supercooled to $-40\,°C$. This is in contrast to that of freezing a bucket of water which normally occurs at less than a few degrees of supercooling. Consideration must be given to the nucleation of concentrated sulfuric and nitric acid mixtures in high level polar stratospheric clouds whose particles can remain liquid to temperatures far below $-50\,°C$.

This study is concerned with understanding the phase change of solution droplets in high level clouds and their subsequent crystal growth. The emphasis is concerned with specific metastability and phase changes, not only in PSC but in all aerosols. In the lower atmosphere the aerosols consist of mixtures of ammonium sulfate, ammonium bisulfate, sodium chloride and others. In the stratosphere, at PSC levels, aerosols are comprised mainly of sulfuric and nitric acid from volcanic injection or from upward diffusion from the lower atmosphere. It is these aerosols that are suspected of catalyzing ozone destruction reactions by adsorption on the surfaces of crystallized particles. For high concentrations of acids, viscosity increases to give the droplet the appearance of a glass at sufficiently low temperatures, limiting the internal diffusion of adsorbed trace components.

Major questions arise concerning the extent to which such particles supercool prior to crystallization, the nature of the crystallization process itself in these droplets, and the nature of subsequent growth from vapor depending on environmental conditions—temperature and vapor pressure. The phase of the particle is important in determining the role these particles serve as either a growth nucleus or a substrate for adsorption/absorption of trace chemical species and heterogeneous catalysis.

Literature pertinent to the formation of PSCs and the physical relationships influencing nucleation and aerosol growth is reviewed. Experiments to exhibit the influences of composition and temperature on nucleation and crystal growth rates for solution of sulfuric acid ($H_2SO_4$), nitric acid, ammonium sulfate, ammonium bisulfate, and sodium chloride are described, together with recommendations for future research.

## CHAPTER 2: THE ATMOSPHERE

The vertical distribution of temperature for a "standard atmosphere" is shown in figure 1. This profile is representative of typical conditions in the middle latitudes. As indicated in the figure, the vertical profile can be divided into three distinct layers: troposphere, stratosphere, and mesosphere. The tops of these layers are called the tropopause, and stratopause, respectively.

The troposphere (literally, the turning or changing sphere) accounts for more than 80% of the mass and virtually all the water vapor, clouds, and precipitation in the earth's atmosphere. It is characterized by rather strong vertical mixing; for example, in clear air it is not unusual for an air parcel to traverse the entire depth of the troposphere over the course of a few days. The transition from the troposphere to the stratosphere is usually marked by an abrupt change in the concentrations of some of the variable trace constituents; water vapor decreases sharply while ozone concentration often increases by an order of magnitude within the first few kilometers above the troposphere. These strong gradients just above the tropopause are a reflection of the fact that there is relatively little mixing between the dry ozone-rich stratospheric and the relatively moist ozone-poor tropospheric air.
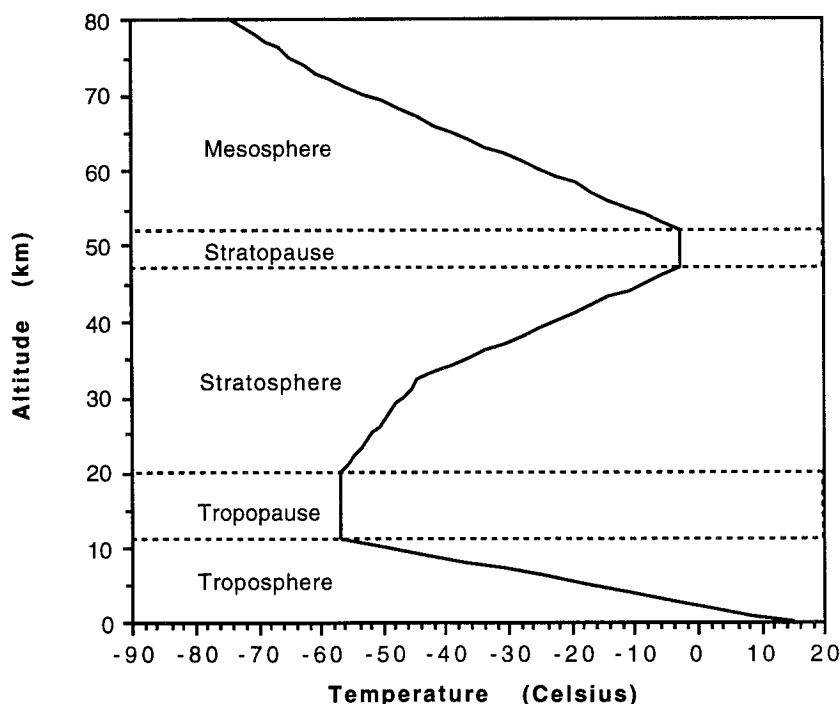


Figure 1. Standard temperature profile. (U. S. Standard Atmosphere, 1976)

The stratosphere (literally, the layer sphere) is characterized by very weak vertical mixing. Aerosols, in stratified layers, are observed to persist for long periods of time within a limited altitude range. It is within the stratosphere where the much publicized and very important protective ozone layer exists. This ozone layer absorbs a large amount of the harmful ultra-violet radiation and prevents it from reaching the earth's surface. Consequently, absorption of the ultra-violet radiation heats the stratospheric air. This absorption is the reason for increasing temperature with height. The temperature maximum generally exists near 50 km. In contrast, during the polar winter months at altitudes of 10–15 km, the lower stratosphere provides the coldest temperatures, 173 K (–100 °C). This study will center on the processes that lead to PSC formation in these regions.

## Observation of Stratospheric Clouds

Stratospheric clouds have been observed for over a hundred years over the poles during their respective winter months. However, with the introduction of the satellite age and the launching of Stratospheric Aerosol Measurement II (SAM II) on the Nimbus 7 spacecraft in 1978, the age of understanding stratospheric aerosol and polar stratospheric clouds began. Detection of clouds was accomplished by the SAM II basic data product—an extinction profile. New investigations have shown that cloud particles are a relatively common phenomena during the Antarctic winters below 25 km, and have a highly negative correlation to temperatures $T < 195$ K (McCormick, et al., 1982). In the past, these clouds were usually observed over land. However, for the first time, SAM II observed clouds where no land existed and which could not be seen from the ground. Researchers were first confused by observance of these clouds at these locations because this eliminated the possibility these clouds were nacreous or mother-of-pearl by nature, which are a form of wave cloud that require mountains for the necessary lift. Also of interest was the equal distribution of clouds throughout Antarctica, Greenland, Canada, and Scandinavia during the polar winters (Steele, et al., 1983). Figure 2 shows a schematic representation of solar occultation, used in determining the extinction as the Nimbus 7 spacecraft passed through sunrises and sunsets at a given altitude.

It was first thought that stratospheric clouds formed rapidly by deposition of water vapor onto sulfuric acid aerosol surfaces when the temperature fell below the frost point of water, approximately –90 °C, as observed with nacreous clouds (Steele, et al., 1983). Extensive work by Mastenbrook in 1968 determined the normal stratospheric water vapor mixing ratio existed around 5 ppmv ($3 \times 10^{-6}$ mixing ratio), or about 1% relative humidity plus an error of measurement. Simple atmospheric models by Hamill, Turco, and Toon (1988) suggest that clouds formed by a 5 ppmv mixing ratio would have an extinction of 0.2 km$^{-1}$ by the time the temperature dropped to 184 K,
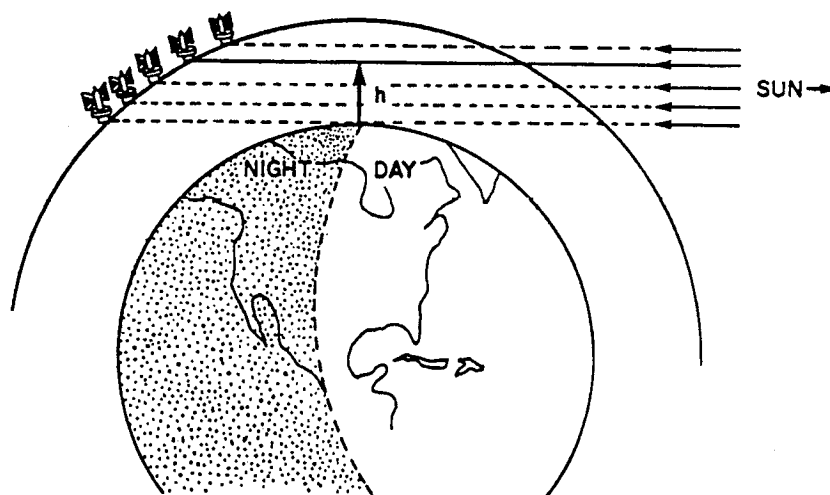


Figure 2. Schematic representation of solar occultation technique employed by the Nimbus 7 SAM II instrument. (Hamill and McMaster, 1983)

4

assuming all aerosols were converted to ice. If only 0.1% of the aerosols grow large, the extinction would range from $10^{-2}$ to $10^{-3}$ km$^{-1}$. Observations of these clouds in the stratosphere by SAM II began to raise many questions on the water vapor content of the stratosphere since data previously obtained by SAM II indicated extinctions between $10^{-2}$ and $10^{-3}$ km$^{-1}$, and only 10% being above $10^{-2}$ km$^{-1}$. However, satellite records for these extinctions only observed temperatures between 190 and 200 K, which is too warm to sustain water ice formation. As a result of the satellite data, these clouds, now considered Type I PSCs, were of considerable interest until it was suggested by Crutzen and Arnold (1986) and Toon, et al. (1986) that these clouds might consist of condensed nitric acid in the form of crystalline nitric acid trihydrate ($HNO_3 \cdot 3H_2O$), a stable form at these temperatures.

As part of ongoing studies into the growth and formation processes of PSCs, it is now believed that this process consists of many stages. The formation and multistage growth idea includes; (1) the precursor stage of supercooled liquid $H_2SO_4 \cdot H_2O$ aerosol (Steele, et al., 1983); (2) an intermediate stage in which $HNO_3$ and $H_2O$ vapors are co-deposited onto frozen aerosol nuclei as nitric acid trihydrate ($HNO_3 \cdot 3H_2O$) (Toon, et al., 1986); and (3) a final stage of coupled deposition of $HNO_3 \cdot 3H_2O$ and pure water ice. Each stage of particle growth is directly related to temperature. To complicate matters, there is evidence that sulfuric acid particles may not freeze at temperatures above 195 K. At these temperatures the particles would be highly supercooled and it is reasonable to assume the formation of a droplet would be comprised of $H_2SO_4$-$HNO_3$-$H_2O$. However, extrapolated values of vapor pressure indicate that very little nitric acid could be incorporated into such particles (Hamill and Toon, 1991).

In 1987, NASA aircraft flew through stratospheric clouds during the Airborne Antarctic Ozone Experiment (AAOE) to collect cloud particles on impactors and filters. Pueschel, et al. (1992) of NASA Ames Research Center, analyzed filters coated with nitron, a precipitating agent for nitrates. The reaction observed with cloud particles and nitron lead to the growth of nitron nitrate, thus confirming the presence of nitric acid in the stratosphere. This study however, was unable to determine whether the polar stratospheric cloud particles were frozen or liquid. It was determined that within the polar stratosphere there exists about 10 times more nitric acid than sulfuric acid. Cadle, et al. (1973) studied the amount of nitric acid present within the stratosphere as a function of latitude and altitude, as figure 3 illustrates.
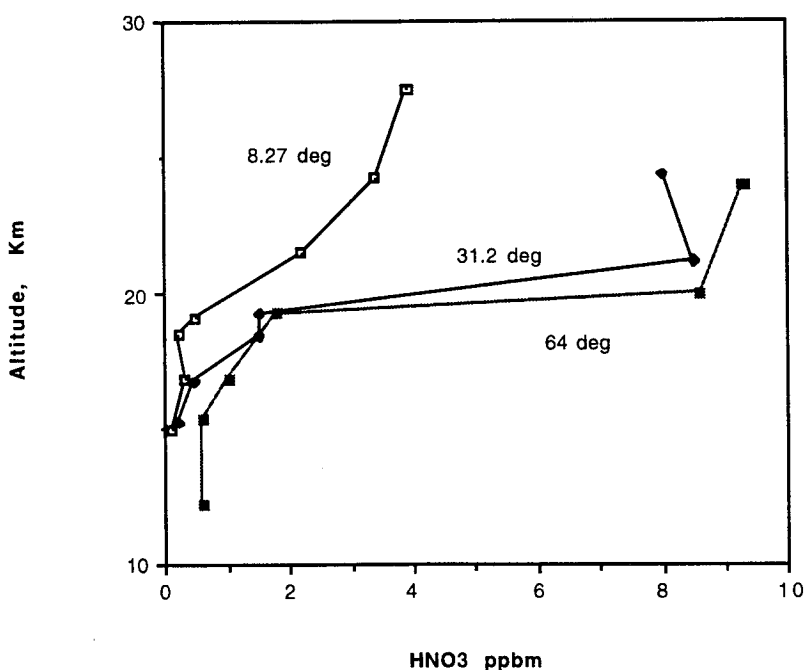


Figure 3. Nitric acid concentration as a function of altitude and latitude. (Cadle, et al., 1973)

# Aerosol Layer

The existence of particles in the stratosphere has been inferred for many years from atmospheric optical effects such as unusual sunsets, mother-of-pearl and noctilucent clouds. The persistence of these optical effects lasting years is explained by a significant amount of particles remaining above the tropopause where downward mixing, turbulence, and washout are nearly non-existent after a major volcanic eruption, such as Mt. Pinatubo in 1991. What has been known is that stratospheric aerosol particles can produce spectacular optical displays such as brilliant sunsets and unusual ring coloration of the sun and moon (Hamill, et al., 1977).

In the late fifties, Junge, et al. (1961) flew a balloon-borne condensation nucleus counter through the 15–20 km levels and discovered that the stratospheric aerosol layer, or Junge layer, was consistent in its behavior and existed world-wide. Since that time, with the aid of improving techniques and better measurement platforms, this discovery was confirmed, although the behavior and consistency, size and concentration, have been proven more variable than was first thought.

The most predominant constituent of stratospheric aerosols, identified by Junge, et al. (1961), is sulfur containing compounds. Particles collected by Junge, et al. (1961) were subjected to fluorescence analysis and found to produce x-ray spectra showing a strong peak at the sulfur K $\alpha$ line, a strong, fairly unambiguous indication of sulfur. Following the 1963 eruption of Mt. Agung, it was discovered that most of the stratospheric particles collected during research were liquid (Rosen, 1964). The most probable liquid at the very low stratospheric humidity was obviously sulfuric acid.

Friend, et al. (1973) suggest the oxidation of sulfur dioxide ($SO_2$) to sulfur trioxide ($SO_3$) with water vapor is the primary formation mechanism of stratospheric particles, $H_2SO_4$. The main source of sulfur dioxide in the stratosphere is from injection of violent volcanic eruptions (Hamill and Toon, 1991) which subsequently became oxidized to $SO_3$. However, with the emergence of the industrial age many anthropogenic pollutants, such as hydrogen sulfide ($H_2S$) and sulfur trioxide ($SO_3$), were released into the atmosphere, providing additional sulfur compounds which eventually were transported into the lower stratosphere. More recently, exhausts of rockets and aircraft have also contributed a variety of gases and aerosols into the stratosphere. Sulfur laden compounds are converted to sulfuric acid ($H_2SO_4$) through photochemical reactions. Appendix A illustrates the photochemical steps in the production and destruction of sulfuric acid as well as thermodynamic and other important properties. When in the presence of enough water vapor and significantly cold temperatures, these vapors will eventually condense, forming small sulfuric acid solution droplets.

Stratospheric aerosol particles are usually found in highly stratified layers beginning near the top of the tropopause and extending up to 30 km or more. The height and thickness of the aerosol layers are quite variable, exhibiting temporal and latitudinal trends, as well as an apparent correlation with tropopause height (Rosen, et al., 1975). The particles are typically 0.1 to 0.3 $\mu$m in diameter and are present at number mixing ratios (NMR, number per milligram of air) of ~60 per milligram (Junge, et al., 1961). In addition, this layer has a marked large particle, >0.3 $\mu$m diameter, and mixing ratio with a maximum located 6–11 km above the tropopause. Figure 4 shows two typical large particle mixing ratio profiles measured at mid-latitudes during 1972–73, showing clearly a maximum in the large particle region. The maximum particle concentration lies in the range of 4–12 per milligram (about 0.4–1.2 particles $cm^{-3}$ at 20 km), falling off to 1.0 per milligram at higher and lower altitudes. This large particle mixing ratio is observed to increase considerably after a volcanic eruption that has plumes penetrating into the stratosphere. However, within 6 months these NMR levels decrease to prevolcanic levels. As observed above, there are significantly more smaller particles than larger particles; however, the larger particles are of more interest since their cross section is responsible for light scattering, and the larger particles act as cloud condensation nuclei.

6
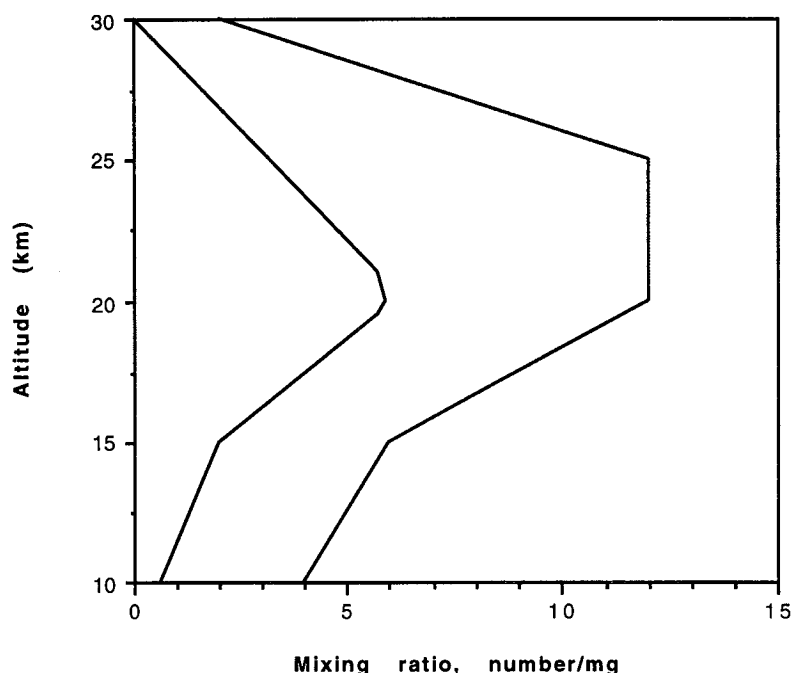
Figure 4. Mixing ratio profiles of large particles, $r > 0.15$ μm, 1972–73. (Hofmann, et al., 1975)

Hamill, et al. (1982) have implied from their research that there must be other sources of particles outside of the stratosphere when volcanic activity is small, providing the nuclei to maintain the Junge layer. Such possible sources are condensed meteoritic vapor and particles transported from the troposphere (Hunten, et al., 1980). Measurements of particles provide evidence against meteoritic vapor below 25 km (Hamill, et al., 1982). Although Hamill, et al. (1982) and others have suggested that the troposphere could provide a source of nuclei for stratospheric aerosols, there is only limited observational evidence for tropospheric particles entering the lower stratosphere (Goodman, et al., 1989). Evidence shows that only $H_2SO_4$ would be produced, and only at the high tropical tropopause where temperatures often reach −80 °C. It is conceivable, however, at these conditions, tropospheric aerosols such as sodium chloride, ammonium sulfate, and ammonium bisulfate may be transported into the stratosphere by the deep convective system within the tropics. At those temperatures these particles may act as condensation nuclei for sulfuric acid vapor. Sodium chloride, ammonium sulfate, and ammonium bisulfate in the troposphere act as cloud condensation nuclei for cirrus and contrails.

## Polar Stratospheric Cloud Formation

Although much is yet to be understood, many new studies are slowly revealing the nature of the formation mechanisms of stratospheric aerosols, nitric acid clouds, and water-ice polar stratospheric clouds. Cloud physicists do, however, consider the important microphysical processes to be nucleation, condensation and evaporation, coagulation and sedimentation. Figure 5 shows steps leading to the formation of the PSC particles. Our interest in these clouds resides mainly in their formation and growth processes and as catalysts for chemical reactions leading to a reduction in the ozone concentrations in the stratosphere (Cadle, et al., 1973).

In the PSC formation process two fundamental questions come to mind. First, how do the background sulfate aerosols serve as condensation nuclei for water and nitric acid vapor (Toon, et al., 1989)? It is presently unclear as to when in the sequence of events the sulfate aerosols become active, providing a nuclei for $HNO_3$ and water droplets. Second, once these droplets form, do they freeze forming nitric acid trihydrate (NAT) particles (Type I PSC) or

7

MICROPHYSICAL PROCESSES

$H_2SO_4$

$O$  $H_2SO_4$  $O$

$O$  $H_2O$

$HNO_3$

$O$

$O$  $H_2O$

$O$  $H_2O$  $O$

$O$

$O$

Cool to ~195K

Cool to ~188K

$H_2SO_4$ aerosol nucleation and growth

Type-I cloud formation

Type-II cloud formation

Sedimentation and denitrification

b

CHEMICAL PROCESSES

$hv$

$CH_4$

$hv$

Cl

HCl

$ClONO_2$

Cooling

$CL_2$ → 2Cl

$O_3$ → 2ClO+2O

$NO_2$

$ClONO_2$

$Cl_2O_2$

$hv$

Photodissociation

Formation of reservoir species

Incorporation of HCl and $HNO_3$ into type-I particles

Repartioning of reservoir species

Catalytic cycle of ozone depletion

Figure 5. Steps leading to formation of PSCs and those leading to the possible ozone destruction. (Hamill and Toon, 1991)

remain supercooled as nitric acid droplets? Type I PSCs are considered by many scientists to be the most important phase in PSC development. It is during this phase of growth that the particles are subjected to additional microphysical processes transforming these clouds into nitrogen sinks, required for ozone destruction. In addition, as temperatures fall below Type I PSCs, deliquescence temperature deposition of water vapor dominates the PSC growth, producing a particle consisting predominantly of water ice (Type II PSC). During this phase, the particles produced can grow large enough to settle out of the lower stratosphere, dehumidifying and denitrifying the stratosphere. Table 1 lists the properties of the stratospheric particles during each phase.

Table 1. Properties of the polar stratospheric particles.

| Composition | Form | Size (μm) | Temp (K) | Location | Source/Area |
|---|---|---|---|---|---|
| 60–80% $H_2SO_4$ (could be as low as 40 wt% $H_2SO_4$) | liquid (perhaps solid also) | 0.01–1.0 | 195–240 | global | OCS* (1 μm²/cm³) Volcanoes (100 μm²/cm³) Aircraft (sulfur in fuels) |
| $HNO_3/H_2O$ (approx 50/50 wt%) (Type I PSC) | solid | 0.3–3.0 | <195 | polar winter | OCS (1 μm²/cm³) $N_2O$ aircraft ($NO_x$) |
| $H_2O$/ice (Type II PSC) | solid | 1–100 (up to 1000 for wave clouds) | <187 | polar winter | OCS (10 μm²/cm³) $H_2O$, $CH_4$ |

*Carbonyl Sulfide (OCS) was coined by Crutzen in 1976, referring to a water-insoluble and chemically inert compound.

Although the stratosphere is much cleaner than the troposphere, it contains a significant amount of suspended particulate matter, namely the aerosol layer containing sulfuric acid droplets. Under normal stratospheric conditions (20 km altitude and 220 K temperature) the sulfate aerosol has an average diameter of about 0.15 μm and a composition of 75% $H_2SO_4$ and 25% $H_2O$. At these temperatures, these particles are most likely to be supercooled liquid drops. Since the relative humidity in the stratosphere is about 1%, it is easy to show that the environment must be cooled to about 188 K before water vapor will condense forming ice crystals.

The equilibrium composition of a droplet of sulfuric acid depends on concentration and temperature. The particles in the stratosphere are constantly being bombarded by vapor of sulfuric acid and water molecules, some of which get absorbed. At the same time, both sulfuric acid and water molecules are evaporating from the droplet. As long as both processes are occurring, the droplet remains in equilibrium. In the stratosphere there are $10^8$ times more water vapor than sulfuric acid vapor, therefore the particle will reach equilibrium with water much more quickly than with sulfuric acid. It is much easier for the droplet to be in equilibrium with water because every time a molecule is absorbed one molecule evaporates. However, when a sulfuric acid molecule is absorbed, the composition changes slightly and the molecule must absorb a water molecule to remain in equilibrium. This leads to a very slow growth by condensation. As the environment turns colder, the droplet becomes more dilute as it absorbs water and grows larger. As the temperature falls during the polar night, reaching <195 K, the droplets swell to nearly twice their original size, and change in concentration from 75% to less than 50% by weight. Figure 6 illustrates the dilution curve of a sulfuric acid droplet with decreasing temperature for a fixed 5 ppmv water vapor mixing ratio (Steele and Hamill, 1981).

Since the droplet is supercooled throughout this entire process, we must consider the possibility that the droplet will freeze before it becomes too dilute. Pruppacher and Neiburger (1963) showed that a solute will enhance the
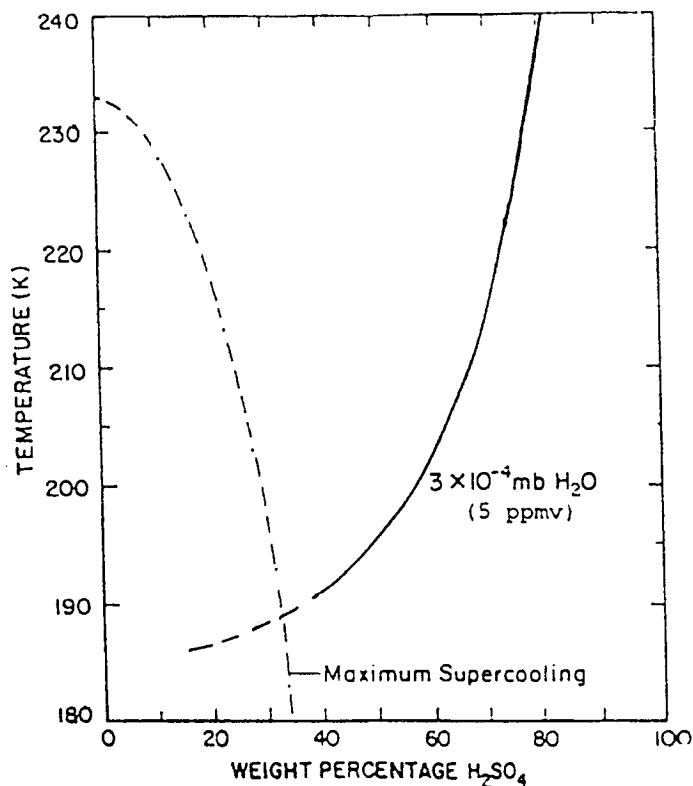


Figure 6. Weight composition and maximum supercooling of sulfuric acid droplet as a function of temperature. (Steele and Hamill, 1981; Hallett and Lewis, 1967)

supercooling of pure water and the resultant supercooling will be the sum of the maximum supercooling and the equilibrium freezing-point depression due to the solute. Hallett and Lewis (1967) assumed the supercooling of dilute sulfuric acid droplets in the stratosphere could be very large. In figure 6, the dashed line shows the Hallett and Lewis curve for supercooled sulfuric acid. Based on the works of Hallett and Lewis (1967), and the change in concentration by Steele and Hamill (1981), homogeneous freezing of sulfuric acid can be expected where the two lines cross, about 189 K. Freezing of the droplet could occur at warmer temperatures by heterogeneous nucleation, i.e., nucleation on a foreign body such as an ice crystal. Crutzen and Arnold (1986) suggest that as the temperature falls below 191 K, the $H_2SO_4/H_2O$ solution droplets will most likely be frozen, forming sulfuric acid tetrahydrate (SAT), based on observation which shows cirrus-like particles near 191 K. Due to their small sizes, there is no direct method to determine if they are in a solid phase. There is an indirect piece of evidence for solid phase; Lidar observations show large polarization values representative of nonspherical particles. This evidence only proves that solid particles are present and fails to prove that liquid particles do not exist.

Shortly after the discovery of the ozone hole in Antarctica in 1985 by Farman, et al., and cloud extinction coefficient observations from SAM II, it was postulated by Toon, et al. (1986), and Crutzen and Arnold (1986), that the PSC cloud observed might be composed of condensed nitric acid trihydrate (NAT) or Type I PSC. Hanson and Mauersberger (1988) in a series of laboratory studies, provided in detail the composition and vapor pressure of the trihydrate and monohydrate at conditions observed in the stratosphere. These studies have led them to the conclusion that the nitric acid trihydrate hydrate is the most stable at stratospheric conditions. Calculations by Toon, et al. (1986) also suggest that the nitric acid monohydrate may be neglected since the ambient $HNO_3$ vapor pressures are much too low for the monohydrate formation at typical stratospheric temperatures. Nitric acid is formed by photochemical reaction of reactive $NO_x$ compounds (NO, $NO_2$, and $N_2O_5$) and water vapor. These compounds are produced by natural and man-made processes. Appendix B illustrates the photochemical equations involved in the production and destruction of nitric acid, along with other important properties of nitric acid.

The growth for Type I PSCs is considered the same as for the sulfate aerosols. That is, they are most likely in equilibrium with water vapor and grow only when nitric acid molecules impinge on the droplet. The formation of nitric acid PSCs in the stratosphere probably does not consist of the freezing of pre-existing supercooled nitric acid droplets. It seems more likely that the PSC evolves from condensation of $HNO_3$ and $H_2O$ vapor onto existing frozen or supercooled particles, most likely of sulfate aerosols. According to Hanson and Mauersberger (1988), the saturation of $HNO_3$ with respect to NAT is expected at temperatures around 195–196 K for normal stratospheric concentrations at 50 mb.

In addition to the nitric acid trihydrate cloud, another type of cloud can form. This type occurs when the Antarctic winter temperatures fall below 190 K. As the air cools, water vapor condenses on some of the suspended particles, forming water-ice clouds (Type II PSC). The seed particles for these clouds are the nitric acid particles, which have themselves grown on sulfuric acid particles. These clouds, although rare, must be given some consideration since it is these cloud particles that grow quite large (10–100 µm). However, they are few in number.

In the stratosphere, prior to PSC formation, the amount of nitric acid in the vapor phase is about 5 ppbv, or 5 times greater than the gas-phase concentration of sulfuric acid (Hamill and Toon, 1991). It is therefore considered that the growth rate and particle sizes of Type I PSC are considerably larger than that of sulfuric acid particle growth. With the observed water vapor concentration of between 2 and 5 ppmv, an even faster growth of Type II clouds exist. In fact, the growth rates for Type I and II ice clouds are so short (hours or less) that their sizes are controlled mainly by the rate of temperature change.

The polar stratospheric clouds are critical to the formation of the Antarctic ozone hole for the following reasons. First, they act to remove nitrogen compounds from the stratosphere by sedimentation, important for the existence of high levels of reactive chlorine species that destroy ozone (Salawitch, et al., 1989). With the particles growing large,

as Type II PSC, more and more nitric acid and water is removed by selective nucleation, whereby only a small number of large particles are produced. It is currently believed that these few large particles slowly sediment out of the stratosphere, removing both water and nitric acid (Salawitch, et al., 1989), taking perhaps a few weeks to occur. Secondly, unreactive forms of chlorine, such as $ClONO_2$, are converted into reactive forms of chlorine on the surface of these clouds (Turco, et al., 1989). Reactions of importance are $N_2O_5$ and $ClNO_2$ with water and $ClN_2O_5$ and $ClNO_2$ with HCl on the surfaces of the PSC producing reactive chlorine and nitric acid. The removal of nitric acid, a Cl neutralizer, by deposition and conversion allows the free Cl atoms unrestricted access to ozone. However, when the sun returns and the PSC evaporate, nitric acid is returned to a gaseous state that slowly photolyzes into $NO_2$, reducing the availability of reactive Cl.

It follows that formation of the number of nitric acid particles cannot exceed the number of sulfate particles, but could be much less dependent on a number of factors. For example, if the temperature decreases slowly, the first nitric acid particle to form could absorb a significant amount of the excess nitric acid retarding nucleation of other particles. Models by Poole and McCormick (1988) suggest that with high cooling rates, 5 K/day, the rate at which $HNO_3$ condenses is small compared to the rate of increase of available $HNO_3$ vapor (i.e., difference between the saturated vapor pressure at the surface and the ambient partial pressure), and thus large supersaturation is created, allowing the activation of most frozen sulfuric acid aerosols. This rate of cooling suggests that tens of minutes are required for PSC to form. For cooling rates less than 1 K/day, $HNO_3$ condensation is balanced for all particles producing fewer nucleated NAT particles. This results in large particles. Hofmann (1990) believed the particles observed in Antarctica are the result of growth in which slow cooling rates were observed.

## Particles in Solution

### Deliquescence

In the next sections, important concepts will be presented to better explain PSC development. It should be noted that **not** all material will absorb water at the same rate. There is a common relationship between vapor pressure of the solution and the concentration of the solute dissolved in the solution. This relationship is known as Roault's law:

$$\frac{e'}{e_s(\infty)} = \frac{n_0}{n_0 + n}$$

where $e'$ is the vapor pressure over the solution containing $n$ moles of solute, and $n_0$ moles of solvent; and $e_s$ is the vapor pressure of the pure solution with no solute dissolved within. The law says that vapor pressure of a solution varies inversely with concentration. With the number of components and phases of this system in thermodynamic equilibrium, there can only be one degree of freedom. Therefore, a solution drop at a particular temperature will be in equilibrium at only one concentration, and one relative humidity (RH). RH is the ratio of vapor pressure over the solution droplet containing the solute to the vapor pressure of the droplet containing no solute. If the relative humidity of the environment were to rise, equilibrium would be shifted and the particle would grow. If the relative humidity were to drop below the equilibrium point, the resultant change would cause the particle to evaporate. This equilibrium point is called the deliquescence point. Not all solutes have the same deliquescence point; some of the relevant ones are summarized in table 2.

### Particle Growth: Influence of Solute

When mixing water vapor and a solute together a variety of things happen, such as the lowering of the vapor pressure and freezing point. However, in discussing such effects we need to first identify the solution products for

Table 2. Relative humidities of phase transition. (Twomey, 1977)

| Particle composition | Observed RH |
|---|---|
| Sodium Chloride (NaCl) | $\approx 76\%$ |
| Ammonium Sulfate (NH$_4$)$_2$SO$_4$ | $\approx 80\%$ |
| Ammonium Bisulfate (NH$_4$HSO$_4$) | $\approx 40\%$ |
| Nitric Acid (HNO$_3$) | $\approx 70\%$ |
| Sulfuric Acid (H$_2$SO$_4$) | $\approx 1\%$ |

which nucleation will take place and to determine the degree of dissociation or association. This is determined by the number of ions which are freed by dissociation or combined in association. For a given solute, the value $i$, the Van't Hoff factor, is given to describe the number of ions each solute will provide to solution. The size of the ions and the solvent both determine the Van't Hoff value; for instance, ammonium sulfate (NH$_4$)$_2$SO$_4$ produces 3 ions, but only 2.3 ions are added to pure water (Low, 1969). A dissolved solute tends to lower the equilibrium vapor pressure of a liquid. Briefly, when a solute is added to a liquid, some of the liquid molecules that were on the surface layer are replaced by solute molecules. In addition, these solute molecules have an attraction force on one another that restricts the movement of the liquid molecules. For this reason the vapor pressure of the liquid is lowered.

For $N_0$, the number of effective solute molecules of mass, $M$, in lowering the vapor pressure may be given by $iN_0M/m_s$, where $m_s$ is the molecular weight of the solute. The number of water molecules in mass, $m$, may likewise be expressed by $N_0m/m_v$. The mass of water, $m$, may be written $4/3\pi\rho_Lr^3$. When these values are combined and rearranged, the ratio then becomes

$$\frac{e'}{e_s(\infty)} = 1 - \frac{3im_vM}{4\pi\rho_Lm_sr^3}$$

or

$$\frac{e'}{e_s(\infty)} = 1 - b/r^3$$

where $b = 3im_v/4\pi\rho_Lm_s$.

Upon inspection of this equation it is obvious that the saturation vapor pressure is decreased proportionally to the number of ions freed in solution, and negatively inversely proportional to the cube of the radius.

## Particle Growth: Influence of Curvature

In a growing droplet, the equilibrium vapor pressure over a droplet surface also depends upon its curvature and is given by (Kelvin term)

$$e_s(r) = e_s(\infty) \exp (2\sigma/rR_v\rho_LT)$$

Here, $e_s(r)$ is the vapor pressure over a surface of radius, $r$; $\sigma$ is the surface tension between the liquid and the vapor; $R_v$ is the universal gas constant; $\rho_L$ is the density of the liquid, and $T$ is the temperature. This means that a droplet of radius $r$ will be in equilibrium in a vapor environment where flat surfaces of a solution are supersaturated. This equilibrium is a metastable one with respect to growth of a droplet because it takes work to grow an embryo to

size $r$, but if an embryo gets larger than $r$, the energy of the system is reduced. This is important because the mechanism for formation of crystals in the atmosphere requires the growth of a drop to a size where nucleation can take place.

Combining the two previous terms produces the Kohler curve, an equation which relates the saturation ratio as a function of particle curvature and the contribution of solute in solution (which by the equation lowers the saturation ratio) as given by

$$\frac{e_s{}'(r)}{e_s(\infty)} = \left[1 - \frac{b}{r^3}\right] e^{a/r}$$

where $a = 2\sigma/\rho_L R_v T$; and for $r$ not too small, a good approximation is

$$\frac{e_s{}'(r)}{e_s(\infty)} = 1 + a/r - b/r^3$$

Figure 7 shows these Kohler curves for sulfuric acid over a range of initial sizes observed in the atmosphere. These curves represent a range from $10^{-16}$ to $10^{-14}$ grams for each solute, and a fixed Van't Hoff coefficient. These curves, which are not the same for all materials, are used to illustrate the sizes of a particular particle at the equilibrium vapor pressure, or relative humidity that exists for a given mass particle. In addition, the curves aid in determining the nucleation point of a droplet at a given molality, an important tool in understanding the nucleation processes that contribute to the formation of PSCs.
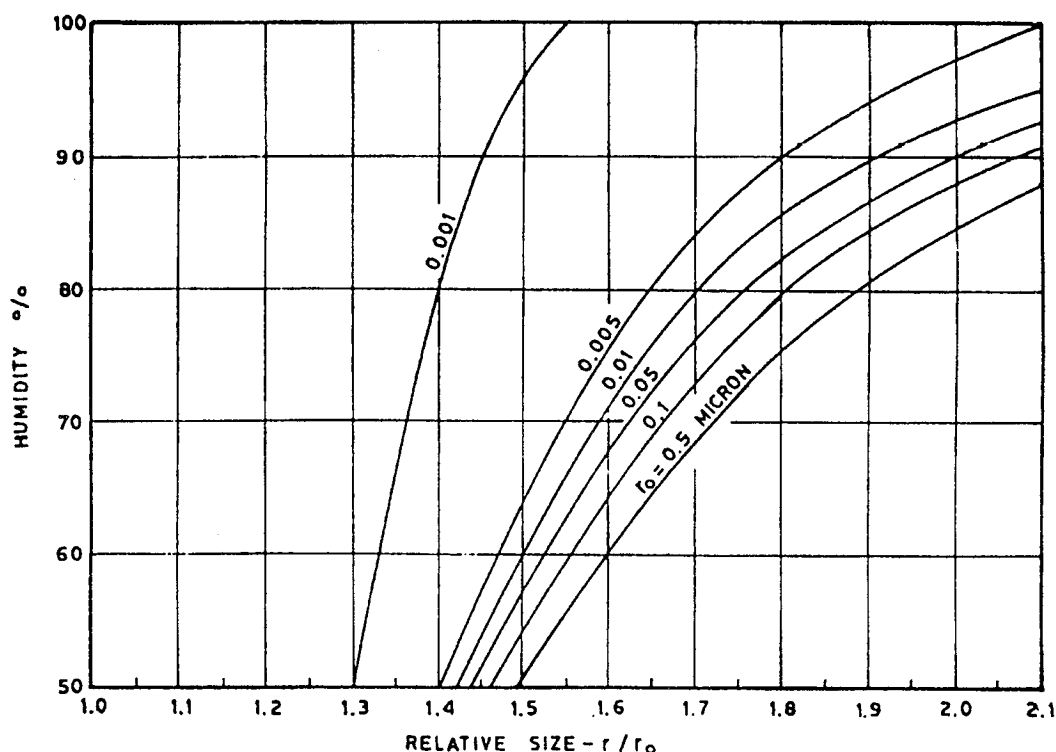


Figure 7. Differences in growth of aqueous solution droplets of $H_2SO_4$. The dry size is indicated on each curve. (Nair and Vohra, 1974)

## Gibbs Free Energy

In order for a particle embryo to form and grow an energy barrier Gibbs Free Energy must first be overcome. The reason the equilibrium is metastable rather than unstable is that the energy barrier must be minimized for this process to occur. During the process of nuclei growth the energy is reduced under experimental conditions. The mechanism of nuclei growth can be analyzed by considering the embryo as a tiny sphere. The sphere will have both volume and surface energies expressed by $E = ar^3 + br^2$. This relationship is shown in figure 8. The first term is the energy needed to create a volume, neglecting surface energy, multiplied by $(4/3)\pi$ for a sphere. The second term is the surface area term, where $b$ is multiplied by $4\pi$ for surface energy. Without going into great detail on the values of these terms, we can show the importance of the terms as a function of changing radius. The equation has a minimum for $r = 0$ and $r = -b/a$, and a maximum at $r = 0$ and $r = -2b/3a$. The value for $b$ will always be positive due to the energy needed to form a surface. The "$a$" term, however, is not as simple. For example, the energy required for a molecule to leave the surface of a sphere would increase the energy of the sphere because the volume would decrease, thus increasing the surface tension to hold the sphere in its shape. Conversely, the energy of a sphere would be reduced when vapor condenses onto a sphere, increasing its volume.

In summary, the value of $a$ is a function of the environment. Where $a$ is positive, work is required to grow the embryo. If the term were negative, as for a supersaturated solution, the embryo would grow rapidly, but only if the critical size were met ($r = -2b/3a$). For $a > 0$, no growth is observed; for $a = 0$, growth is possible; and for $a < 0$, growth is certain.

## Effects of Relative Humidity

In the atmosphere a wide range of relative humidities can be encountered, from 1% in the stratosphere, to saturation, and on rare occasion supersaturation. The non-soluble particles are silica, dust, oils and a variety of other
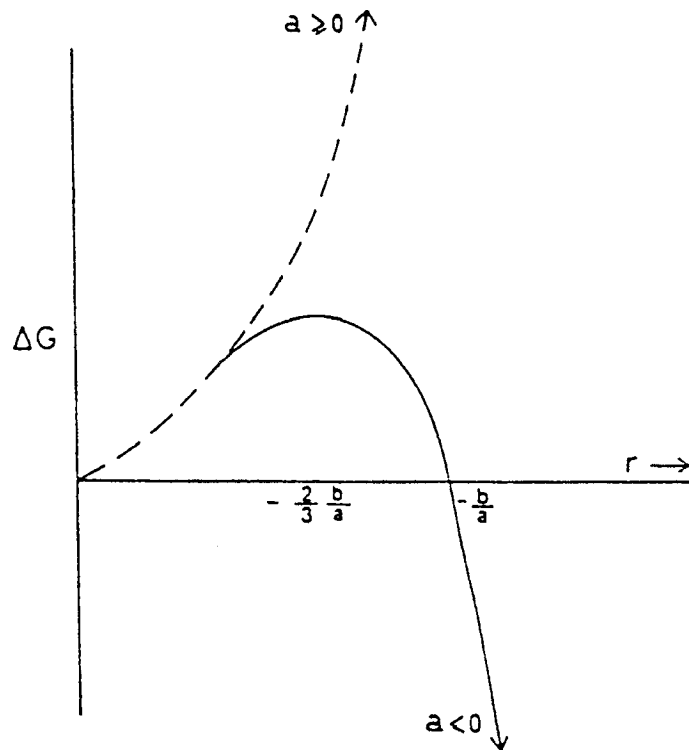


Figure 8. Gibbs free energy plot showing the critical radius growth. (Twomey, 1977).

material. The soluble particles are ammonium sulfate and sodium chloride, existing in size ranges of >0.1 and >1.0 μm. The physics of these particles are especially important to cloud and fog formation for visibility and corrosion.

The phase rule of physical chemistry states that the equilibrium of a system of C components and P phases possesses C – P + 2 degrees of freedom. For a system of a soluble salt and water vapor, three phases exist; a solid, an aqueous solution, and water vapor with two components (water and salt). The degree of freedom is one, which means that we specify one thermodynamic variable, temperature; the other variable factors are set and not free to vary. In other words at a given temperature, water vapor, solution, and solid can exist at only one vapor pressure or relative humidity. Therefore, this relative humidity represents a phase transition point or a phase transition line on the temperature-humidity diagram. Figure 9 shows the equilibrium relative humidity line of a saturated solution against temperature.

## Growth Rate Factors

Studies have shown crystal growth should occur at the rate of diffusion; however, the rate has been shown to be slower (Humphreys-Owen, 1949). In fact, growth rates were observed to change discontinuously. In crystal growth theory there appears to be three main factors to influence growth rates: diffusion, release of latent heat, and viscosity. While the driving force of crystal growth is diffusion, latent heat and viscosity work against the process, providing a balance of forces and equilibrium.

The principal assumption in growth models is that it happens very fast. The limitation in the rate of crystallization is the transfer of solute from solution to the crystal. This transfer process ordinarily involves an eddy of molecular diffusion. This rate, considerably slower than for pure solvent, is believed to be caused by the hindering of the molecules as they traverse the medium toward the crystal (O'Hare and Reed, 1973).
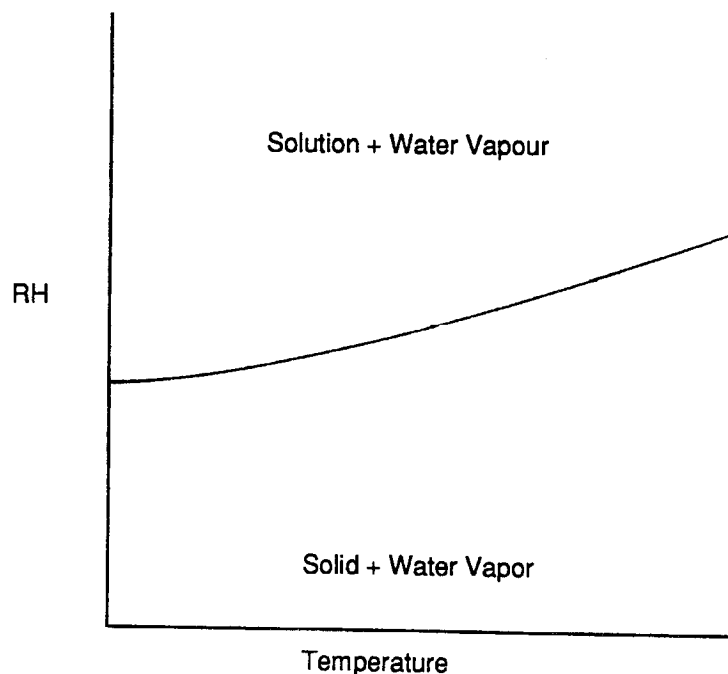


Figure 9. Equilibrium relative humidity (RH) line of a saturated solution against temperature—a curve which also represents the transition line between the regions of solid and solution. (Twomey, 1977)

15

Lindenmeyer, et al. (1957) showed ice crystal growth in pure water was limited by the amount of latent heat released, demonstrating the transport mechanism most responsible for the removal of the thermally enhanced reaction products. Hallett (1964) showed that ice crystal growth in supercooled water grew at a rate approximately equal to the square of the supercooling.

Another limiting factor in the growth rate of crystals is viscosity. Viscosity is related to the solute, its characteristics, and the environment. In general, most solutions become viscous when the temperature is reduced. It is very clear that if a solution is a highly viscous solute, molecules may not be able to diffuse to the growing crystal quickly enough and the growth will be very slow. For a viscous solution, the growth rate of a crystal can be described by

$$V \approx \frac{1}{\eta} \Delta T^n$$

where $\eta$ is the viscosity, $\Delta T$ is the degree of supercooling, and $n$ is the power having a value of 1 or 2 (O'Hare and Reed, 1973). For example, if one lets honey sit for a few months, crystal growth can be observed. If the solution concentration increases the viscosity enough, it is conceivable, in theory, that growth rate would not increase and may actually slow down, and effectively cease.

## What the Experiment Will Show

Through the years in which the polar stratospheric particles have been studied, there still remains confusion whether the PSC exists as highly supercooled liquid droplets, frozen sulfate particles, or particles in a highly viscous glass transition. The interest of these experiments is to better understand the phase transition of the particles as they move from stratospheric aerosol to Type I and then to Type II PSC. The transition phase of these particles may be the key in determining the rates at which $O_3$ is being destroyed.

The experiments were conducted to provide detailed data concerning the composition, phase, and formation processes of PSCs. To understand the possible phase behavior, sulfuric and nitric acid, ammonium sulfate, ammonium bisulfate, and sodium chloride solutions were supercooled and nucleated to observe solution growth rates at stratospheric temperatures. These growth rates were explored over a wide range of temperature and solution concentrations. In addition, military aircraft exhaust (soot), provided by NASA Dryden Flight Research Center (DFRC), Edwards, California, was added to these solutions, re-supercooled and nucleated to investigate any changes in growth rates due to the addition of the soot. In the stratosphere, mixing of this soot may be neglected due to the stability and the lack of turbulence; it is therefore possible that these particles may require a very long time before eventually falling out. For example, a 1 $\mu$m particle, large for a stratospheric aerosol, has the fall speed of about 0.13 cm sec$^{-1}$, requiring a matter of weeks for fallout. Some consideration should be given to this theory if the PSCs are observed more frequently in the future due to the ever increasing amount of exhaust being transported into the stratosphere, or directly injected there.

A significant portion of the experimental work consisted of attempts to simulate a glass phase of $H_2SO_4$-$H_2O$ and $HNO_3$-$3H_2O$ solutions by supercooling small volumes, 0.04 ml, of solution. This glass phase assumes, at extreme supercooling, the volume is transformed into a highly viscous liquid or glass without crystal growth. These experiments were conducted in a controlled environment to measure the crystallization rate.

## CHAPTER 3: EXPERIMENTAL PROCESS

The experimental setup was designed to measure the crystal growth velocities of solutions at different concentrations and degrees of supercooling. In order to investigate these properties, an experimental setup similar

to that of Yang and Good (1966) and others was used. This consists of a "|__|" shaped clear glass tubing of different bore diameters, having identical test observation sections and overall column lengths. Each piece of tubing is approximately 30 cm, having a sample interval of 15 cm, and a test interval of 7 cm in length. This is illustrated in figure 10. These experiments use 6 different bore hole diameters (0.5, 1.0, 2.0, 4.0, and occasionally 5.0 and 6.0 mm). The tubing size choices were determined so that the dimensions of the glass tube opening were large enough to allow either an ice crystal or a liquid nitrogen cooled wire to be easily inserted. Secondly, minimization of the volume of liquid was desired in order to achieve maximum supercooling. This setup was chosen because it was a simple setup with few moving parts and allowed a good view of the growing crystals.

A Neslab model 220D cooling bath with adjustable temperature control, to -90 °C, was selected. The system provides an enclosed coolant containment basin in which the glass tubing setup with solution sample could be immersed. Cyrocool® from Savant Inc., (a clear silicone based heat transfer liquid) was chosen because of the low temperatures required, -55 °C. This particular liquid remained less viscous than any other heat transfer liquids reviewed, and at -90 °C, Cyrocool remained less viscous than water at -90 °C. When choosing a heat transfer liquid, it was important to consider the viscosity trends as a function of temperature. Cyrocool met these requirements.
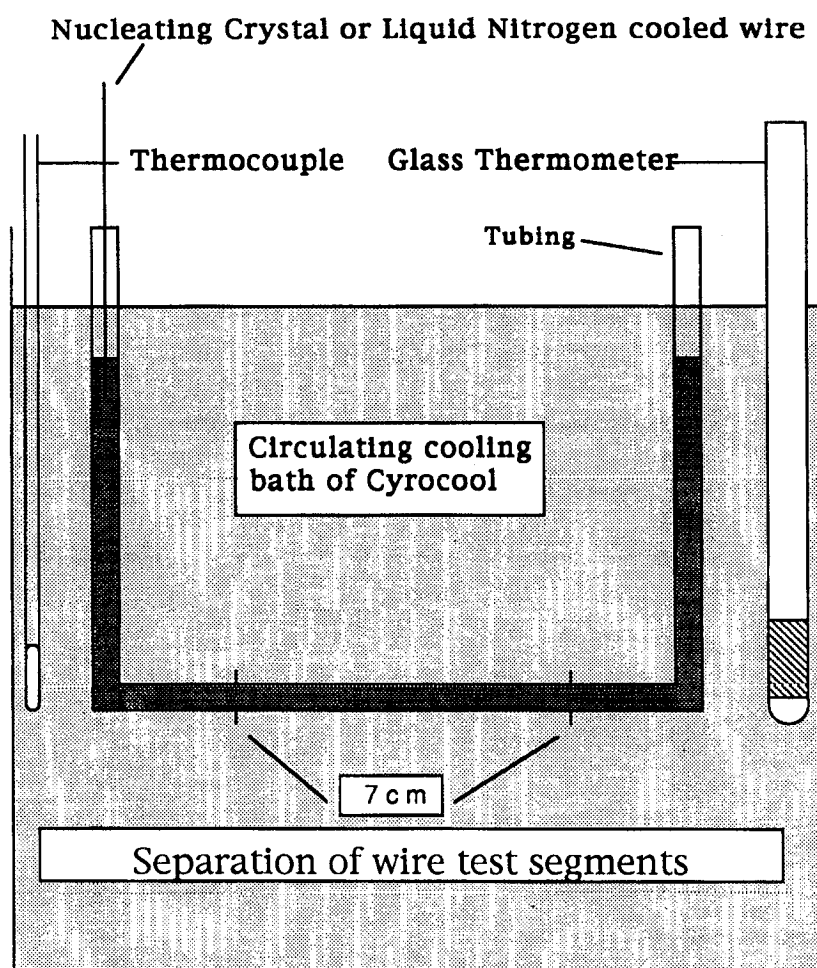
**Nucleating Crystal or Liquid Nitrogen cooled wire**

Thermocouple    Glass Thermometer

Tubing

Circulating cooling bath of Cyrocool

7 c m

Separation of wire test segments

Figure 10. Illustration of the experimentation setup.

For accuracy and repeatability the temperatures were monitored by a calibrated thermocouple, to ±0.05 K, and an accurate mercury thermometer, to ±0.1 K. The thermocouple and thermometer were connected to the apparatus at opposite ends as illustrated in figure 10, five centimeters below the surface. This arrangement was used so that the liquid could be monitored for the possible formation of thermal gradients, which could lead to erroneous results.

## Characterizing the Solutions

Solutions of different concentrations, ranging between 1 and 5 $m$ (molality, $m$ = moles of solute per kilogram of solvent), were prepared using standard techniques for each of the 3 salts (<5 $m$) and the 2 acids at dilute concentrations (<3.5 $M$, molarity, $M$ = moles of solute per liter of solution). For acid concentrations greater than 1 $m$, the concentrations are referred to in molarity, instead of molality. The solutions were prepared to ±0.05 $m$ using certified American Chemical Society (ACS) grade sodium chloride (NaCl), ammonium sulfate ($(NH_4)_2SO_4$, ammonium bisulfate $(NH_4)HSO_4$, and reagent grade ACS sulfuric acid 98.8% ($H_2SO_4$) and nitric acid 70% ($HNO_3$). The salts were poured into a beaker filled with warm distilled water, and stirred by a Gyratherm magnetic stirrer for about 1 hour. The acids did not need to be stirred by the magnet, but were shaken periodically to ensure complete mixing. At the higher concentration for nitric and sulfuric acids, the freezing point depression, $\Delta T_f = K_f m$ (Glasstone and Lewis, 1960) where $K_f$ is the freezing point depression constant, was not very meaningful. This will be shown later by the equilibrium curves for sulfuric acid by Gable, et al. (1950), and for nitric acid by Pickering (1893). The solutions were prepared with distilled water and placed into containers that had been thoroughly cleaned with strong detergent, rinsed with distilled water, and placed on a clean shelf to dry.

## Supercooling the Solution

This particular cooling device had a built-in mechanical circulating system which constantly mixed the fluid at the desired temperature, usually between –3° and –55 °C, keeping any temperature gradients to a minimum. During this phase of the experiment the maximum supercooling for each solution at each concentration was determined by slowly cooling the sample until only self nucleation occurred with the solution almost in equilibrium. Thermal equilibrium for the setup was established according to the time constant equation given by Carslaw and Jaeger (1959):

$$\tau \approx \frac{r^2}{\kappa}$$

where

$r$ = radius of the tubing, cm

and

$\kappa$ = thermal diffusivity of glass or liquid, $cm^2 sec^{-2}$

Appendix C shows the thermal conductivity, density, specific heat, and diffusivity of a number of substances. The time constant value needed for equilibrium to be established, $\tau$, is equal to $1/e$ or 63.2% of desired temperature value. Thermal equilibrium is established at 5 times $\tau$, which is within 1% of the actual temperature. An estimate of the time required for equilibrium, assuming $r = 3.0$ mm and $\kappa = 5.8E-03$ for glass, the equation shows that $\tau$ equals about 2 to 10 sec, and some 5 times longer for water, depending on the wall thickness. For these studies 3.5 minutes was considered the time to reach thermal equilibrium. Upon reaching thermal equilibrium, and in the absence of premature nucleation, the temperature was decreased by additional 1 or 2 degree increments and allowed to reach equilibrium again. This was continued only until self-nucleation was observed, indicating the last temperature with no nucleation as the temperature limit for supercooling.

As a comparison, several tubing sizes (0.5, 1.0, and 4.0 mm diameter) were prepared with identical solutions to identify the effects of tube size on supercooling. It is believed that the size of the sample volume, the type of solution, and the material of the tubing is important in determining how much supercooling can be possible. This study was conducted using only a 1 $m$ solution of ammonium sulfate.

Experimental care was used to minimize potential problems. For example, during these experiments several problems involving the glass tubing were observed. Namely, the glass had flaws that induced premature nucleation. In addition, if the tubing was not properly cleaned after a test run, residual material may have been left to nucleate the next runs early in the supercooling process. Also the solution, although carefully prepared, may have had some impurities that affected both the supercooling and growth rates.

## Crystal Growth Rates

This setup was ideal for establishing the growth rate characteristics of the solutions to identify and observe the following properties: crystal growth velocity and crystal shape as a function of supercooling, temperature, and concentration. The growth velocity $V_r$ (cm/sec), is defined as the velocity of the moving solid-liquid interface in a supercooled or supersaturated solution. First, the growth rate for a 1 $m$ ammonium sulfate solution was conducted using the 0.5, 2.0 and, 4.0 mm diameter tubing for temperatures ranging from –4 °C to self-nucleation. This procedure was conducted several times, and the rates averaged to eliminate inconsistencies in timing the growth front passages due to either errors in the timing procedure or errors due to unseen gradients. The timing of these growth fronts was accomplished with the use of an ordinary stop-watch. The starts and stops were determined by visual inspection and still photographs. Photographs were taken to show the crystal shapes at low and high supercooling. The timing started as the growth front passed one of two wire markers on each tube and stopped when the front passed the second wire. During this portion of the experiment it was important to have accurate knowledge of the temperature of the coolant immediately surrounding the tubing setup. This was necessary in order to minimize temperature gradients within the solution prior to nucleation. For this reason the temperature was consistently monitored at both ends of the apparatus.

Secondly, the crystal growth rate experiments for each solution at the desired concentrations were conducted in the 0.5 mm diameter tubing. The 0.5 mm bore hole tube was selected since larger supercoolings were observed during the supercooling phase. A volume of 0.04 ml supercools more than a 2 ml volume in accord with the following idea: for given volume there exist a finite number of nuclei that will initiate nucleation. If the volume is halved, the number of nuclei is halved. In theory, if the halving process continues, at some point the volume left will be completely free of any nuclei which could initiate crystal growth. The nucleation of these solutions was initiated one of two ways after reaching equilibrium. First, an ice crystal suspended on the end of a 0.5 mm copper wire was submerged into the supercooled solution just below the surface. Second, if the ice crystal failed to nucleate the solution, the wire was cooled by liquid nitrogen and again submerged just below the solution surface. In most cases this worked successfully. Since the temperature of maximum supercooling was known, the tubing setup, with solution, was submerged in the coolant at a predetermined temperature and allowed to reach equilibrium before nucleation was initiated. Timing of the growth fronts were again conducted the same as before.

Once completed with the initial test runs for solutions <5 $m$, inspection of the crystal growth pattern for higher concentrations of nitric and sulfuric acid occurred. Sulfuric acid and nitric acid each have a series of hydrates which can form depending on the temperature and concentration. For example, at 10% by weight $H_2SO_4$ there exists, if nucleated, solid ice plus liquid $H_2SO_4$. On the other hand, if 100% by weight $H_2SO_4$ were to nucleate, there would exist solid $H_2SO_4$. Within the 10–100% range, there exists many combinations or hydrates of $H_2SO_4 \cdot nH_2O$. These hydrates have a point on a curve where the liquids and solids have the same composition and are in equilibrium with each other. This point, is the congruent melting point of the compound, and allows the solid and liquid with the same composition to coexist.

## Mixed Solutions

Additional experiments were performed to determine the affects on the supercooling and growth rates from mixing identical concentrations of sulfuric and nitric acid. As shown earlier, the particles observed as PSC contain both sulfuric and nitric acid in different proportions. These experiments investigate the affects, if any, due to the mixing of these two acids. Since the phase of the Type I PSC was known to contain significantly more nitric acid than sulfuric acid, ratios of 80% and 95% by volume of nitric acid were mixed with 20% and 5% by volume of sulfuric acid. The solution mixtures were prepared using a 1 and 3 *M* concentration of each solution. The procedures by which the maximum supercooling and growth rates were conducted were identical to the previous experiments.

## Aircraft Soot Mixtures

A follow-on experiment examined a small amount, 0.6 grams per 15 ml solution, of engine exhaust (soot) added to the 3 *M* concentrations of nitric and sulfuric acid, 95/5 and 80/20 respectively. This experiment simulated the possible interaction between stratospheric aerosols, cloud particles, and insoluble aircraft exhaust. This soot was exhaust buildup of JP-4 fuel from an engine of a F-104 Starfighter, an aircraft capable of flying to 70,000 ft. The soot for these runs was obtained by scraping residue from the rear of the exhaust nozzles of the aircraft. This particular aircraft had not been used for at least 6 months and it was unclear as to the exact composition and what additional materials (such as sand, metal, smoke, etc.) that may have been contained in the residue. This aircraft, considered one of the dirtiest burning engines, puts many grams of soot aerosols per pound of fuel into the atmosphere. The interest of soot may be important due to the increase of the nucleation rate of aerosols leading to the production of aircraft contrails and early nucleation of stratospheric aerosols, a precursor to the PSCs. The procedures were identical to those used to determine the growth rate of acid concentrations with no soot.

## CHAPTER 4: EXPERIMENTAL RESULTS

Supercooling is the reduction of temperature of any liquid below the melting point of that liquid's solid phase—that is, cooling beyond its nominal freezing point. Results from the various experiments are displayed in this section. Data plots are presented showing the effects of tube diameter on growth rate and degree of supercooling. Crystal growth rates are plotted as a function of supercooling and temperature for the selected acid and salt solutions. These plots all show good experimental data. Also, three series of photographs showing the growth fronts and crystal shapes at intervals during the course of the experiments under specific conditions are presented.

## Growth vs. Tube Diameter

The use of different size glass tubes or capillaries provided the intended data array. Growth rates as a function of supercooling and tube diameter differed with the larger diameter (4.0 mm) tubing, which has an environment more conducive to higher crystal growth rates. That is, the diameter of the tubing was large enough to allow the crystals to grow in a semi-free environment, free of container walls. On the other hand, the smaller diameter tubing (0.5 mm) restricts the growth rate, which appears to be strongly influenced by tube diameter. Figure 11 shows the effects of tube diameter on growth velocity for a supercooled 1 *m* solution of ammonium sulfate at a temperature of –11 °C (7.3 K supercooled). This trend shows a direct relationship between tube diameter and growth rate. Similarly, figure 12 shows the growth rates and degree of supercooling as a function of temperature and tube diameter. While the 4.0 mm tubing does support a faster growth rate, the 0.5 mm tubing provides for an additional 5 degrees of supercooling, due to a small volume. This was a compromise that will be discussed later. Since this study is mainly interested in simulating the high degree of supercooling experienced in the real atmosphere, the 0.5 mm tubing, with its small volume, was used to provide these conditions. Upon further inspection of figure 11, it appears at some point above 4.0 mm that free growth rate may approach a constant.
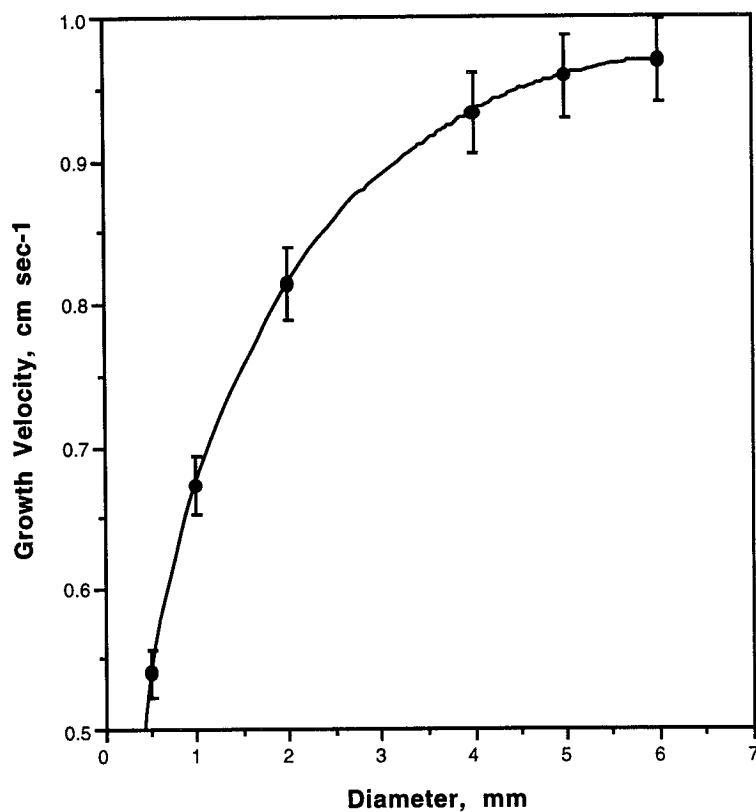
Figure 11. Tubing diameter in supercooling for 1 *m* solution of ammonium sulfate at a temperature of about –11 °C (7.3 K supercooled).



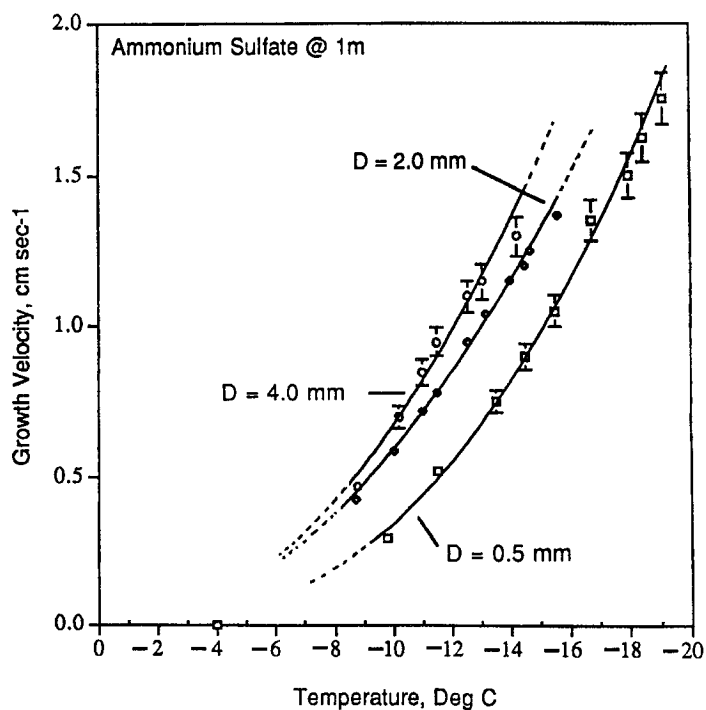Figure 12. Growth rates as a function of tube diameter and temperature. Equilibrium ice-solution temperature is shown at –4 °C.

Data from the larger tube provided important information not obtainable from the smaller tubing—a good view of the growing crystal shapes. Figures 13(a through i) show the growth front within the 4.0 mm tubing containing ammonium sulfate at low, medium, and large supercooling. The crystals observed growing in a small supercooling, <5 K, resembled long thin hollow columns. Crystals that grow in a small supercooling often grow at angles up to 90° from the tube axis and are often difficult to observe. The medium supercooling, 9 K, had crystals that grew along the sides slightly faster than through the middle, showing a more organized structure of growing plates, similar to feathers; this was observed in figures 13(b and c). The larger supercooling, >12 K, had a growth front with crystals growing from the middle shaped like small plate crystals. Figure 13(j) show the shapes of the crystals for dilute solutions experienced over a range of supercoolings (Wedum, 1979). These crystals represented growth in weak sodium sulfate solutions.
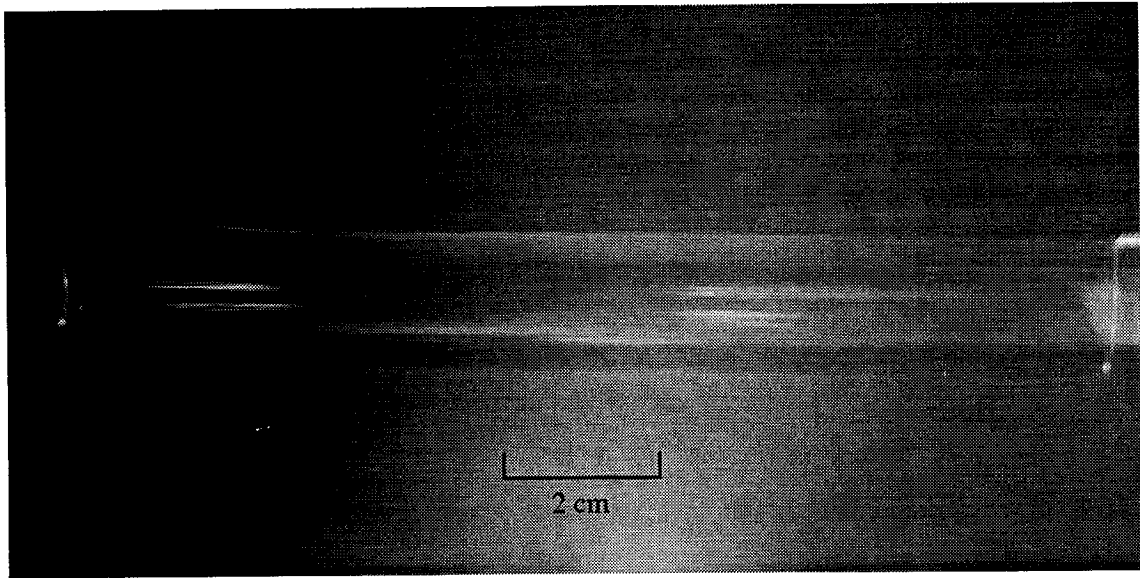


Figure 13(a). Crystal growth of a 1 *m* solution of ammonium sulfate in a 4.0 mm diameter tube at 4.0 K supercooled at 7 sec.
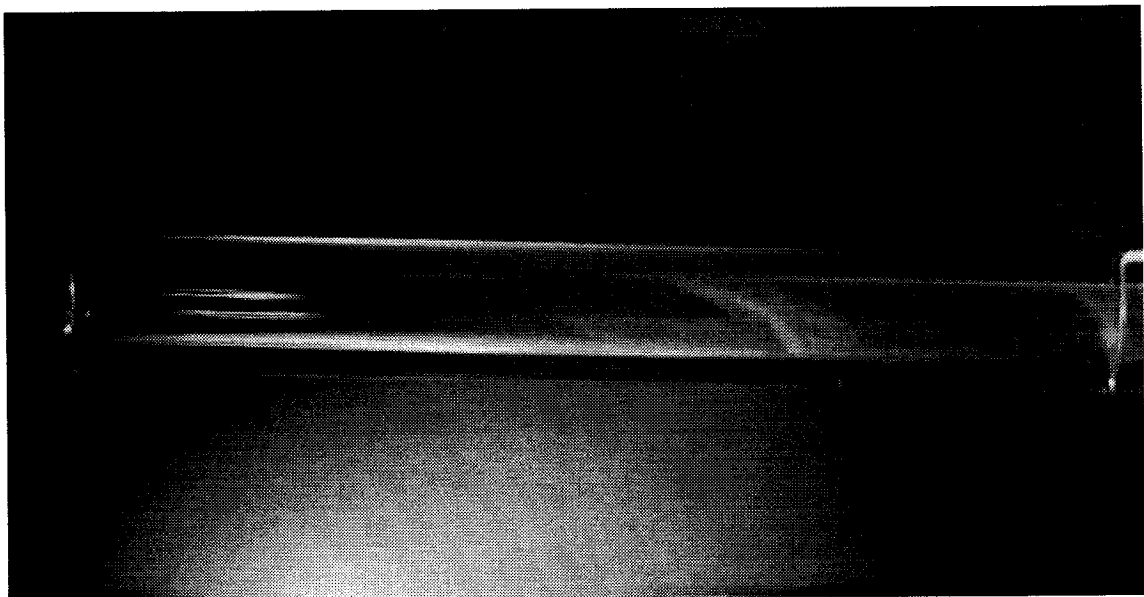


Figure 13(b). Crystal growth of a 1 *m* solution of ammonium sulfate in a 4.0 mm diameter tube at 4.0 K supercooled at 11 sec.
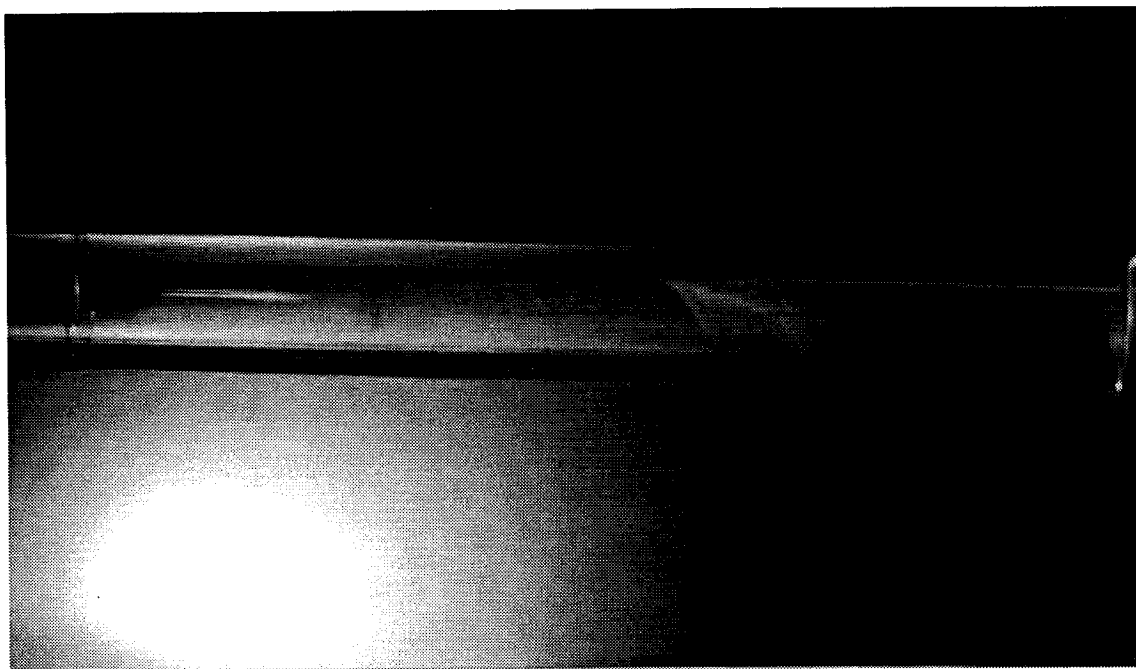
22

Figure 13(c). Crystal growth of a 1 *m* solution of ammonium sulfate in a 4.0 mm diameter tube at 4.0 K supercooled at 16 sec.
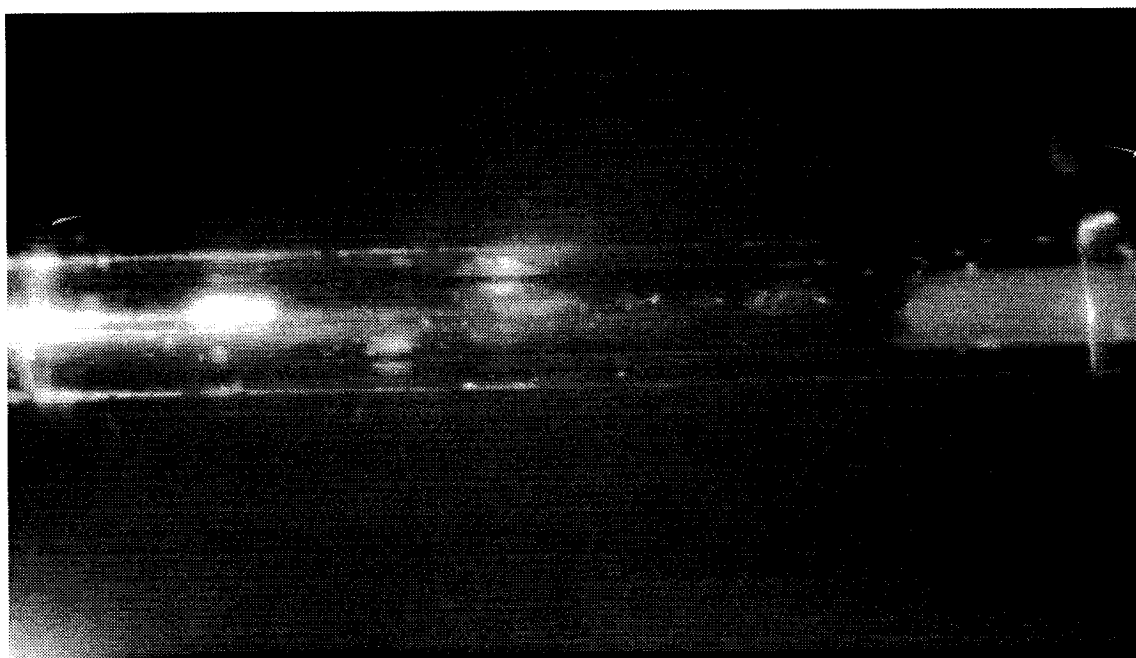


Figure 13(d). Crystal growth of a 1 *m* solution of ammonium sulfate in a 4.0 mm diameter tube at 9.0 K supercooled at 2 sec.
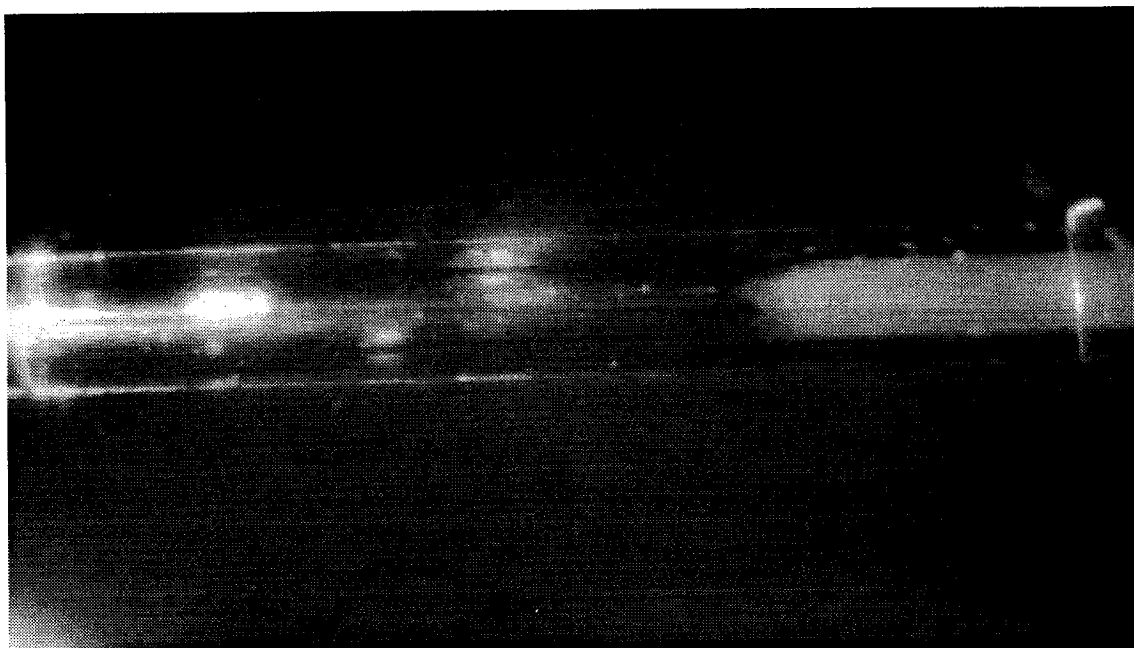
Figure 13(e). Crystal growth of a 1 *m* solution of ammonium sulfate in a 4.0 mm diameter tube at 9.0 K supercooled at 4 sec.



Figure 13(f). Crystal growth of a 1 *m* solution of ammonium sulfate in a 4.0 mm diameter tube at 9.0 K supercooled at 6 sec.

24

Figure 13(g). Crystal growth of a 1 *m* solution of ammonium sulfate in a 4.0 mm diameter tube at 12.0 K supercooled at 1 sec.



Figure 13(h). Crystal growth of a 1 *m* solution of ammonium sulfate in a 4.0 mm diameter tube at 12.0 K supercooled at 2 sec.

Figure 13(i). Crystal growth of a 1 *m* solution of ammonium sulfate in a 4.0 mm diameter tube at 12.0 K supercooled at 4 sec.
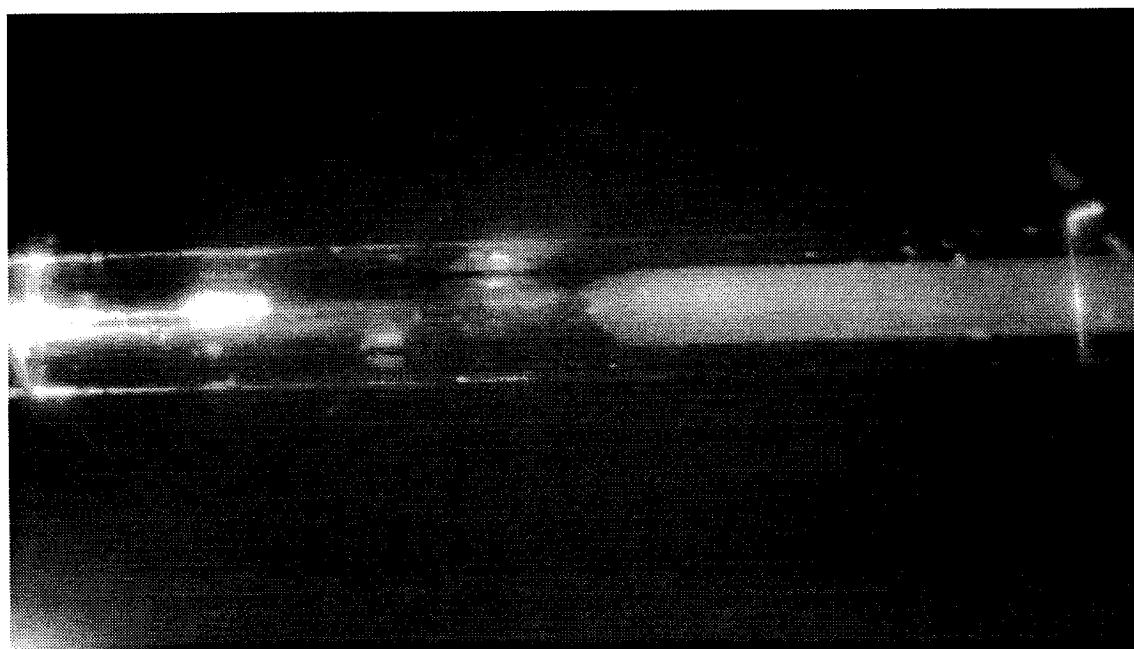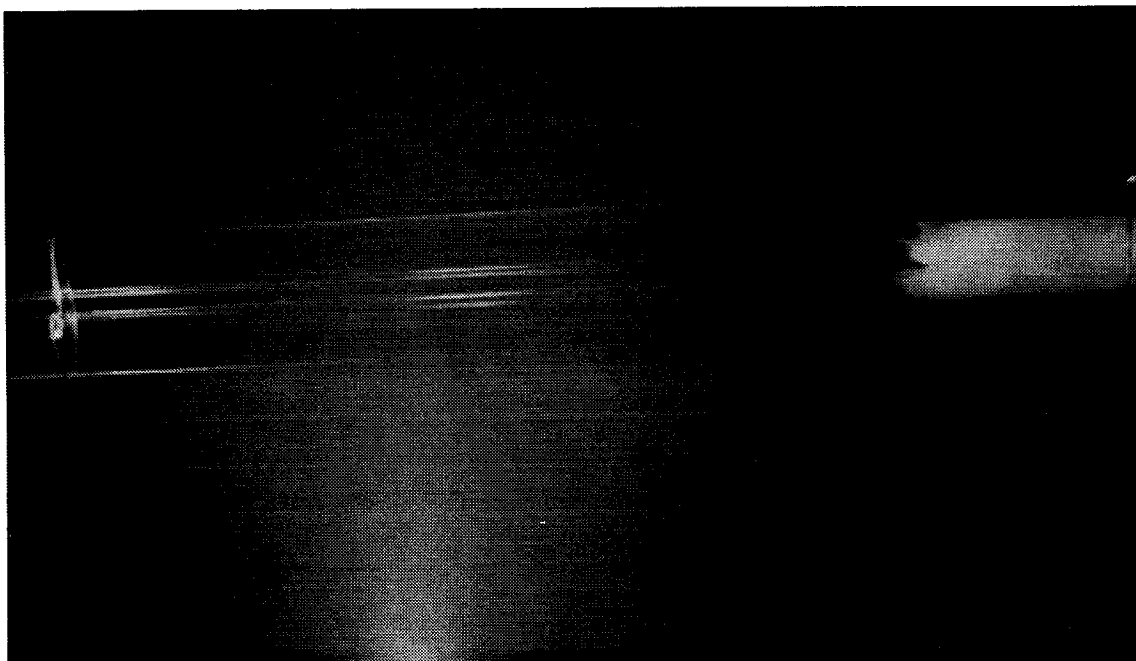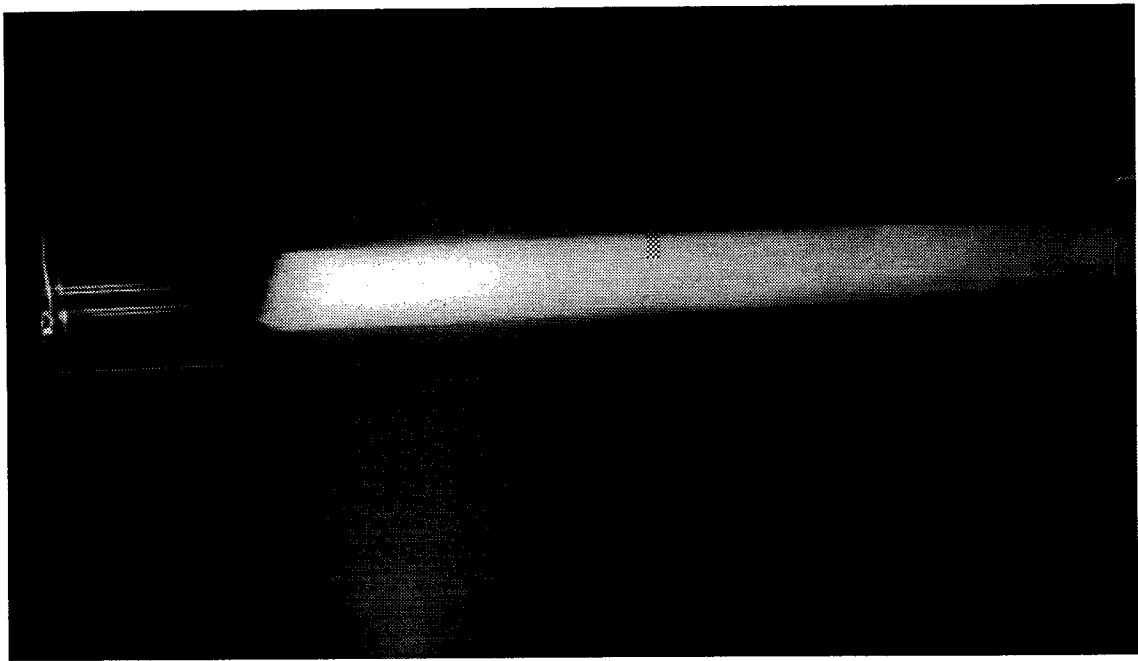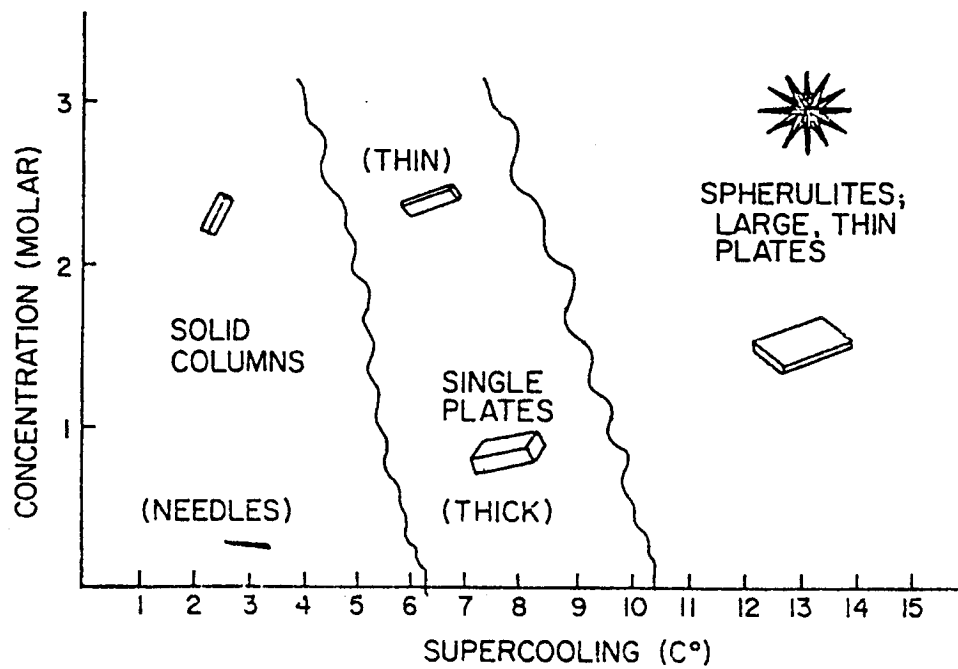


Figure 13(j). Crystal shapes as a function of concentration and supercooling. (Wedum, 1979)

26

During the stage of determination of the growth rates for weak solutions, interest was expressed in observing how the growth rates varied with each run. These runs were conducted 10 times. Data for each run was plotted (figs. 14 and 15) as a function of total time for a low (5 K) and high (10 K) supercooling using the 0.5 mm tubing. These plots show good agreement between each run to 4.0% for the higher supercooling and approximately 5.0% for lower supercooling. The variability was not significant because human error in timing the growth fronts may provide the largest part of this variability.
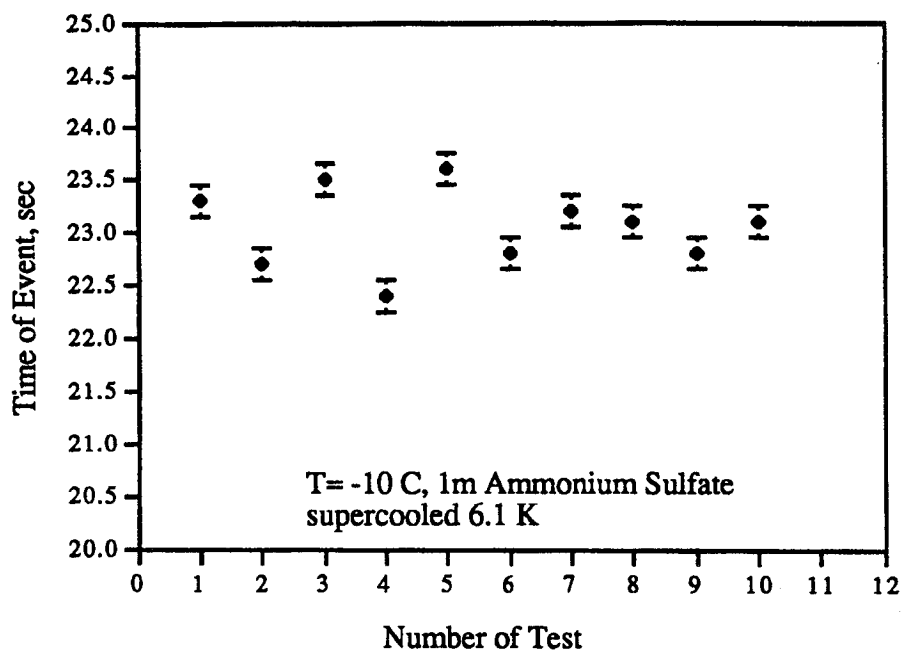


Figure 14. Growth rate errors due to uncertainties in stop-watch timing at low supercooling.
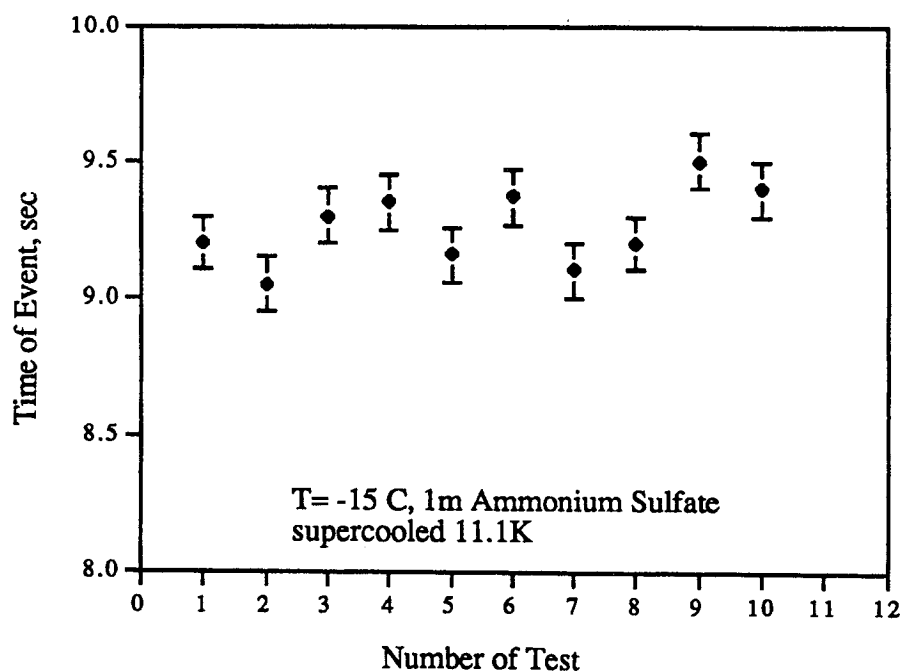


Figure 15. Growth rate errors due to uncertainties in stop-watch timing at high supercooling.

## Salts

The sodium chloride and ammonium sulfate experiments were successful and predictable, particularly due to the ease and stability of these substances in solution. It should be noted that sodium chloride and ammonium sulfate are solubility-limited at extremely cold temperatures and have a finite solubility at any temperature (*International Critical Tables*, 1922). Figures 16 and 17 show the growth rates of each salt against temperature for each concentration with equilibrium points (zero supercooling) from *International Critical Tables*, 1922. Also displayed are curve fit lines for each concentration. It should be noted that all the plots have the first few curve fit data points eliminated from the figures, the reason being that the growth rates for the first few degrees of supercooling showed a large degree of variability from one run to another, which require greater study. It is clear that at small supercoolings and molality, the crystallization velocity increases with supercooling. This is consistent with earlier results, as is the decrease with molality for a given supercooling (O'Hare and Reed, 1973).

As a solid, ammonium bisulfate is very hygroscopic (taking up water vapor) when left in the open for any period of time. Ammonium bisulfate in solution also takes up water vapor from the atmosphere, and therefore care must be taken when handling and storing. Similar problems exist for sulfuric acid solutions. Not much data could be found for ammonium bisulfate with the exception that it nearly completely dissociates when put into solution, becoming
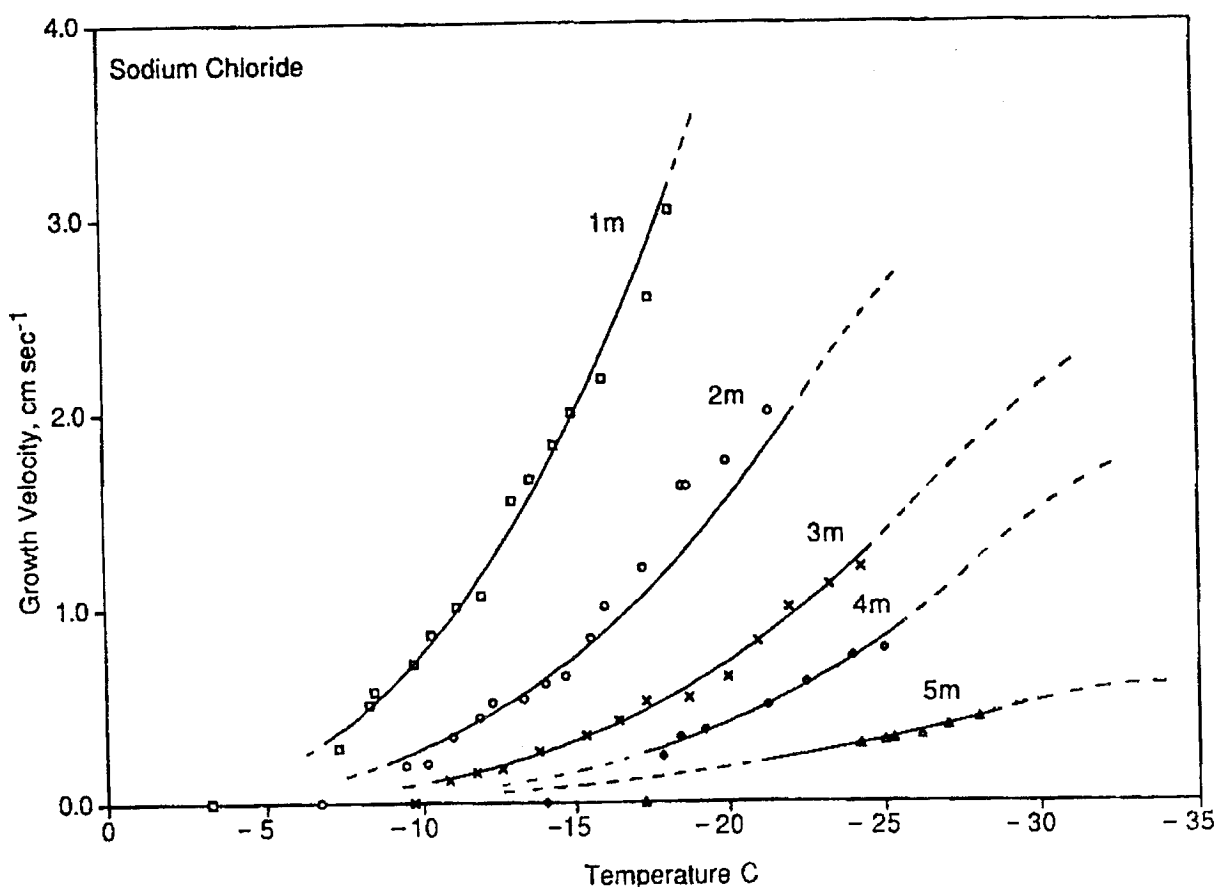


Figure 16. Growth velocity as a function of molality and temperature for sodium chloride; freezing point depression is 3.37 K per 1 *m*.
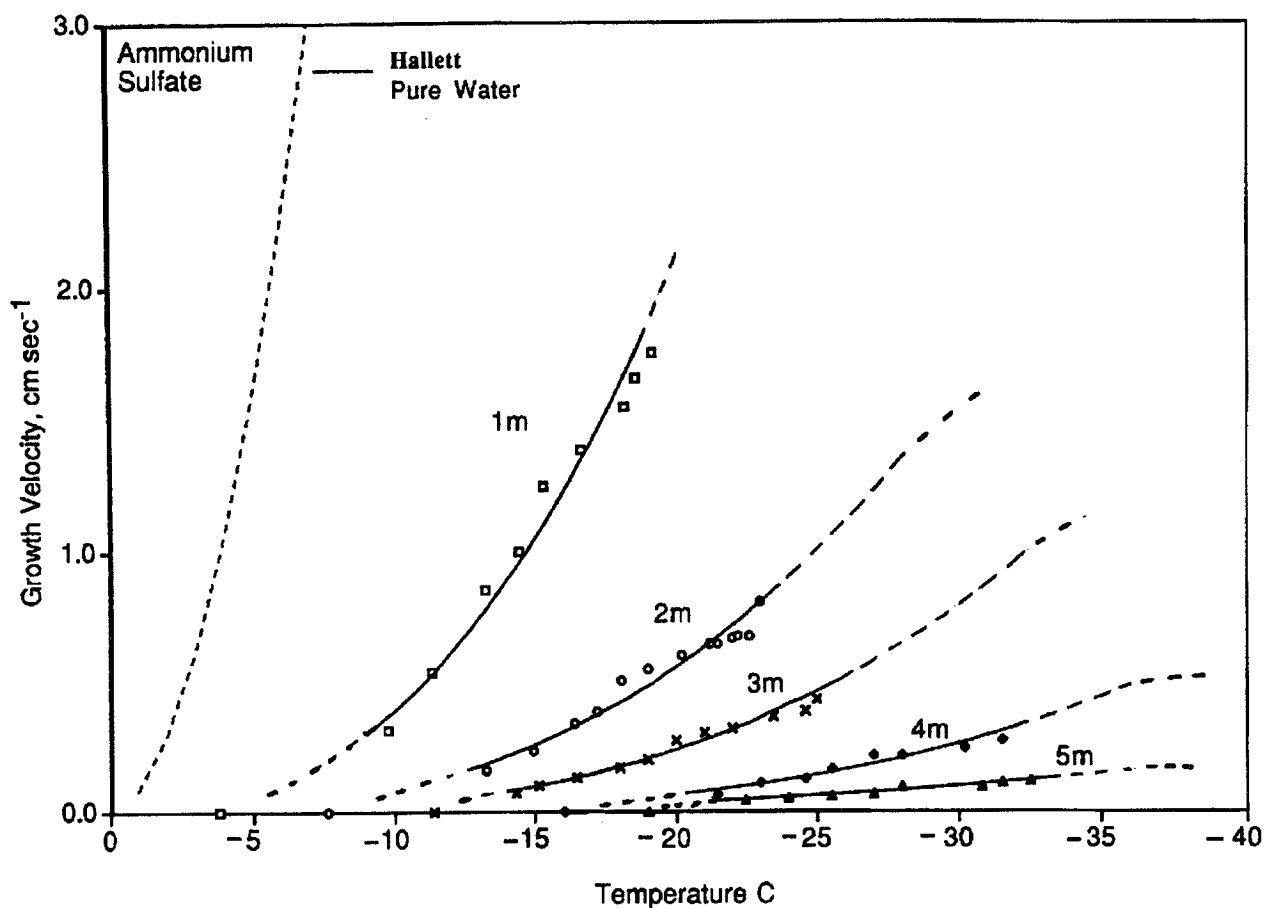
Figure 17. Growth velocity as a function of temperature and molality for ammonium sulfate; with growth rate for pure water; equilibrium freezing point depression is 3.86 K at 1 $m$.

dilute sulfuric acid. Figure 18 illustrates the growth curves for each concentration. These curves are similar to the sodium chloride and ammonium sulfate for weaker concentrations, but at higher concentrations a larger supercooling can be achieved with a much colder self nucleation temperature. Also the growth rate curves begin to show signs of a constant growth rate with decreasing temperature. Since ammonium bisulfate produces a weak sulfuric acid solution, this means that when the solute comes out of solution there is no longer any simple way of determining which crystal is growing, or if the crystal is of purely one substance (either ice or sulfuric acid hydrate).

## Acids

Unlike the salts, the acids are a little trickier to work with, but are infinitely soluble within the temperature ranges of these experiments, -4° to -54 °C. Figures 19 and 20 provide the growth rates for nitric and sulfuric acid. Also illustrated are the curve fits of the data. These data show that the growth rates for the weakest solutions are nearly the same as for the salts. However, for the higher concentrations (2 $m$ and greater) the growth rates are reduced significantly. On these figures, the point farthest to the right for each curve represents the maximum supercooling that could be achieved.

At the higher concentrations and increased supercooling it is clear that as the growth rate slows it approaches a maximum. This is indicative of the increased solution viscosity. The key to this study is the growth rates at the high
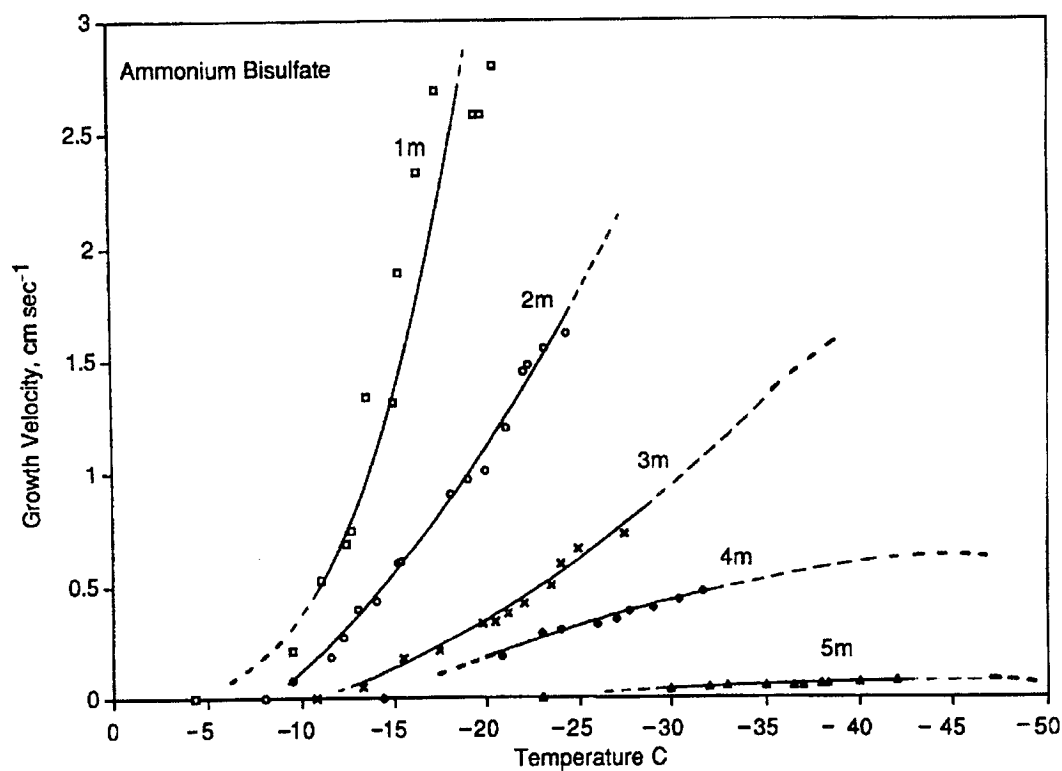
Figure 18. Growth velocity as a function of temperature and molarity for ammonium bisulfate; freezing point depression is 3.8 K at 1 $m$.
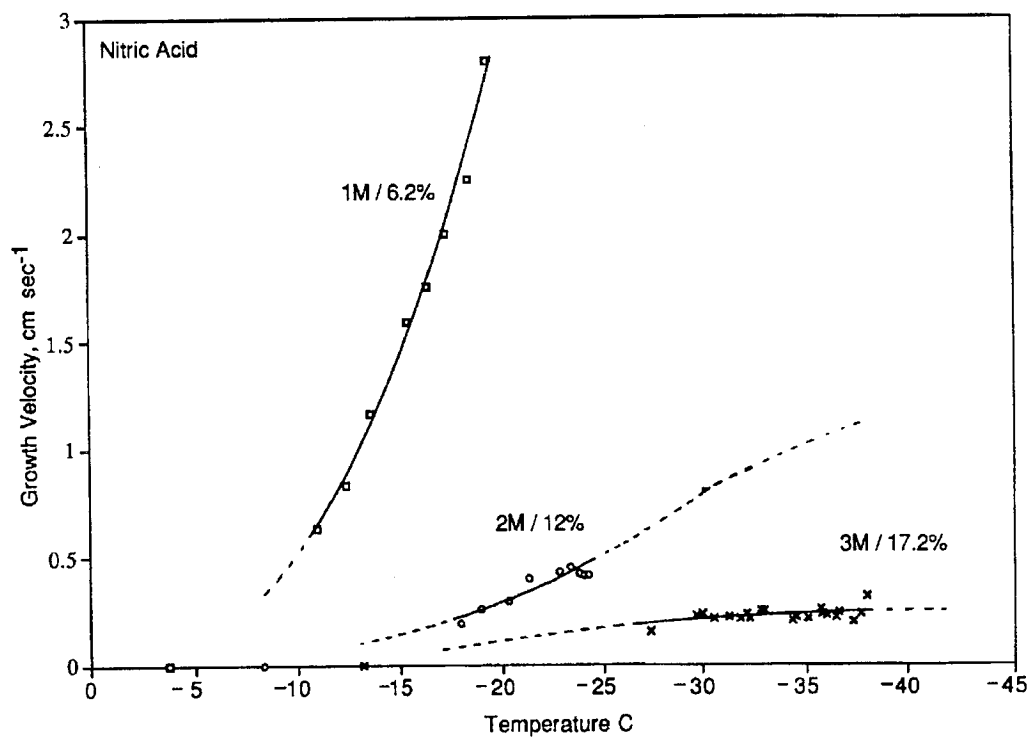


Figure 19. Growth velocity as a function of temperature and molarity for nitric acid; freezing point depression is 3.6 K at 1 $m$.
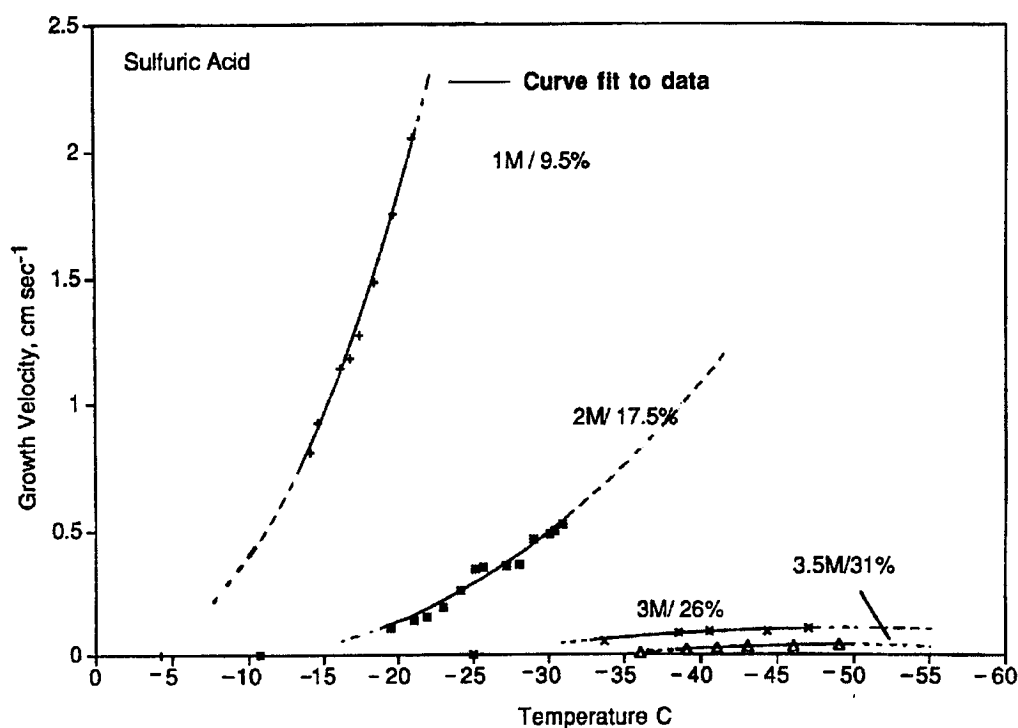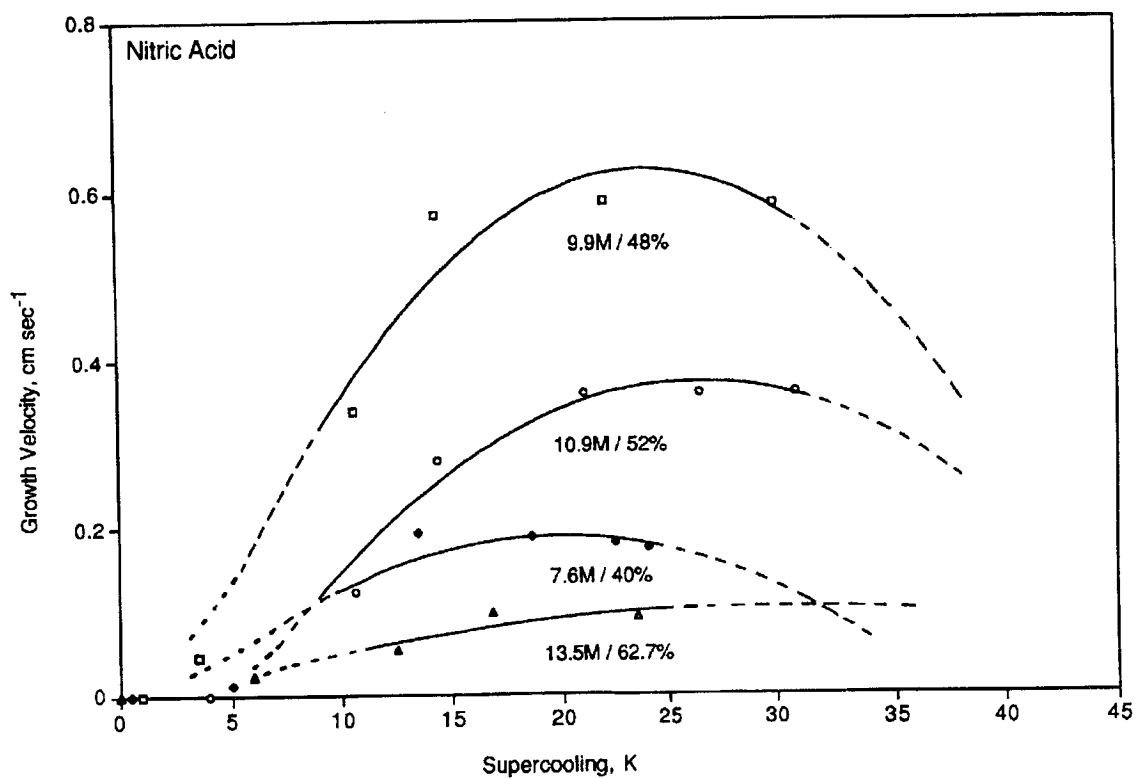
Figure 20. Growth velocity as a function of temperature and molarity for sulfuric acid; freezing point depression is 3.8 K at 1 $m$.

end of supercooling with increased concentration. The curve fit data trends show that if the temperatures could be reduced further providing a higher supercooling, a reduction in growth rate should take place. Extrapolating the growth rate for the acids by 20 K supercooling illustrates nearly a 20-fold decrease in growth rate with a small increase in concentration, from 1.0 to 3.0 $M$.

## Growth Rate at High Concentration

The growth rates observed for higher concentrations are similar to those at lower concentrations, except that the velocities are more influenced by temperature and concentration (i.e., viscosity). Figure 21(a) shows the growth rates for the higher concentrations of nitric acid. These curves show a trend that is generally unclear; for example, the weakest concentration has the coldest equilibrium temperature and the second slowest growth rate. It should be remembered that for the higher acid concentrations the use of molarity ($M$) instead of molality ($m$) was used. As the concentration increases, the equilibrium temperature increases, as does the growth rates. Figure 21(b) shows the growth rate for hydrate crystals as a function of molarity for supercoolings of 10, 20, and 30 K. This can be seen on figure 22 where the two concentrations, 9.9 $M$ and 10.9 $M$, have the same equilibrium temperature. While both have nearly the same equilibrium temperature, the growth rate for the higher concentration is slightly slower, as was expected since more solute is present. The growth rate at the warmest temperature and weakest concentration, 48% by weight ($M = 9.9$), is found to actually have the fastest growth rate. Conversely, the slowest growth rate has the highest concentration and the coldest temperature, 62% by weight ($M = 13.5$). Figure 22 illustrates the equilibrium freezing points for nitric acid from Pickering (1893) and all freezing points for specific concentrations measured during this study. This figure graphically illustrates the location of the temperatures from data in figures 19 and 21.

Sulfuric acid in our study, unlike nitric acid, becomes very difficult to nucleate when concentration rises above 3.5 $M$. In this study 3.5 $M$ was the last concentration to be nucleated, partly because no growth was observed at the

31
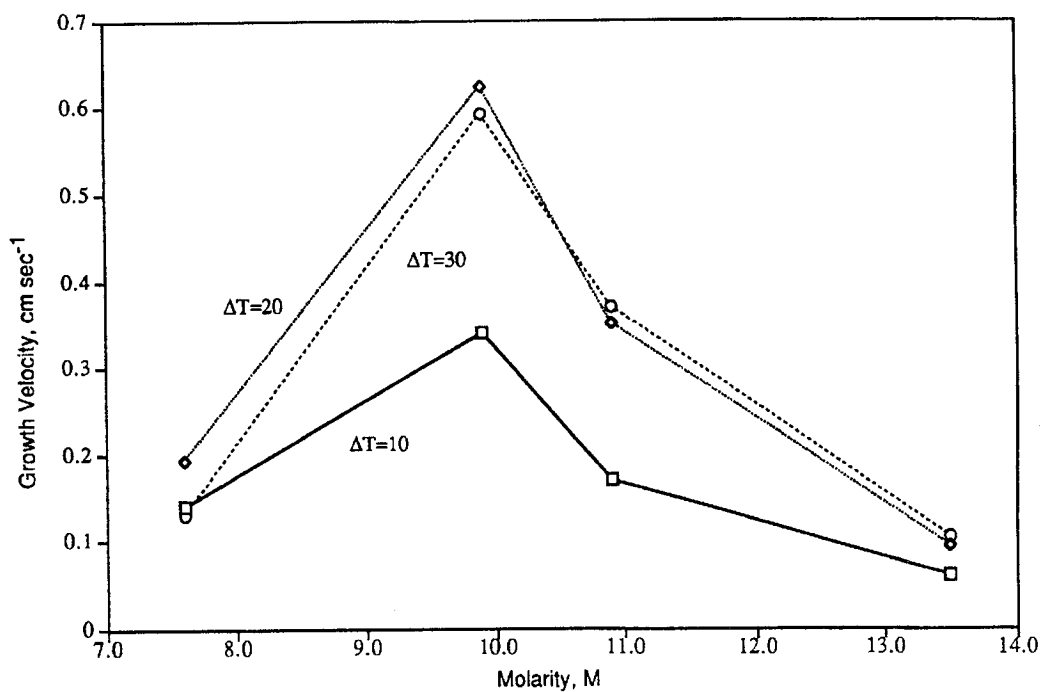
(a) Nitric acid.



(b) 3H$_2$O hydrate crystals.

Figure 21. Growth velocities for nitric acid and 3H$_2$O hydrate crystals as a function of supercooling and molarities. Equilibrium temperatures are –30 °C for 40%, –20 °C for 48%, –20 °C or 52%, and –22 °C for 62% by weight. (Pickering, 1893)
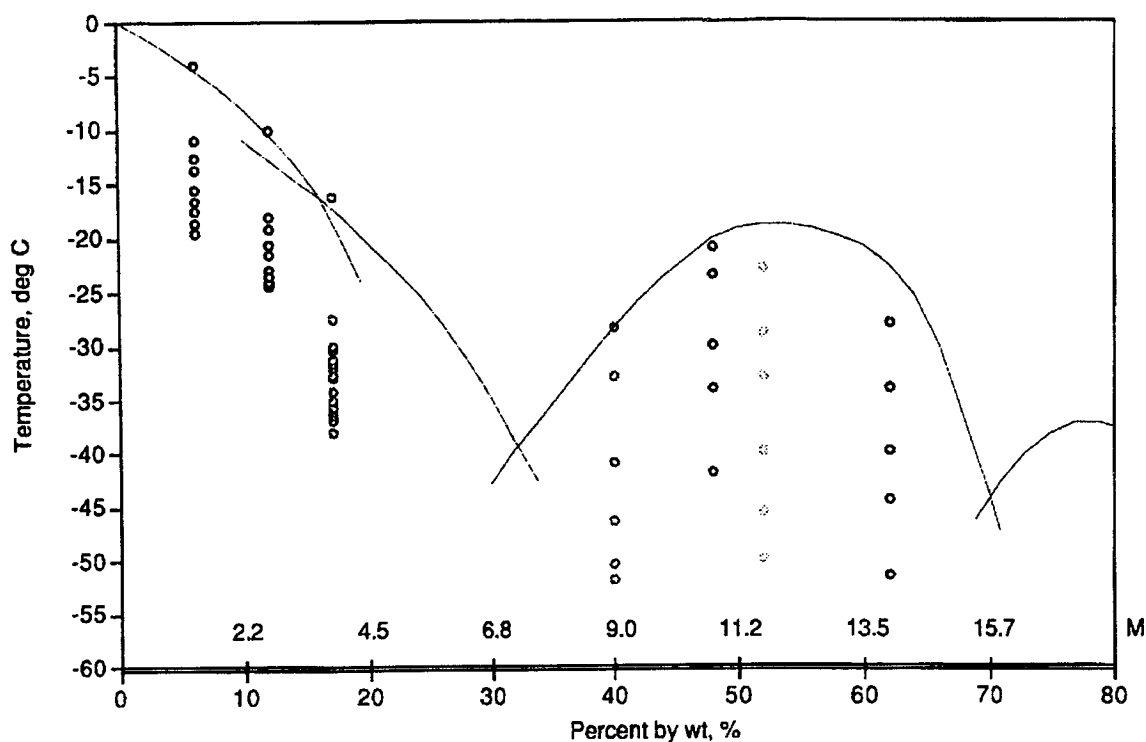
Figure 22. Equilibrium freezing temperatures and experimental data showing temperatures and molarity where nucleation was initiated. (Pickering, 1893)

next higher concentration, and because our equipment could not obtain sufficiently cold temperatures. At these temperatures, sulfuric acid became highly viscous. This is shown in appendix A where sulfuric acid became very viscous with a slight decrease in temperature, which will be discussed later. Figure 23 illustrates the equilibrium freezing curve of sulfuric acid solution by Gable, et al. (1950) with freezing and measurement points from the survey. This figure also presents data showing we were unable to nucleate concentrations above 35% by weight at temperatures the equipment could attain.

## Mixtures of Acids

Much is generally known about sulfuric and nitric acid independently but information on the behavior of their mixtures is needed to understand PSC formation processes. Studies show that they behave very differently in the presence of a cold environment. The supercooling procedure remained identical to that used for the unmixed solutions. Sulfuric and nitric acids were mixed, making two concentrations and each concentration having two different mixtures: 5% $H_2SO_4$ to 95% $HNO_3$ and 20% $H_2SO_4$ to 80% $HNO_3$ at 1.0 $M$ and 3.0 $M$. The growth rates observed were quite uniform, and as expected, the growth rates increased with supercooling. This was observed for both the 1.0 $M$ and 3.0 $M$ concentrations. A surprise was that the growth rates for the mixtures were higher than for the 1.0 $M$ and 3.0 $M$ solutions of sulfuric and nitric acid independently; figures 24 and 25 show these results. Each growth rate test was conducted several times and the results averaged. Again, the curve fit line intentionally deleted the first few less precise data points. These growth rate curves provided show what appears to be a dependence on the concentration of sulfuric acid. For example, the growth rate for the 3.0 $M$ 95–5% nitric is generally higher than for 80–20% nitric at the low supercooling, and at the larger supercooling the growth rate is significantly higher. The same description can be made for the 1 $m$ concentration growth rates.

33
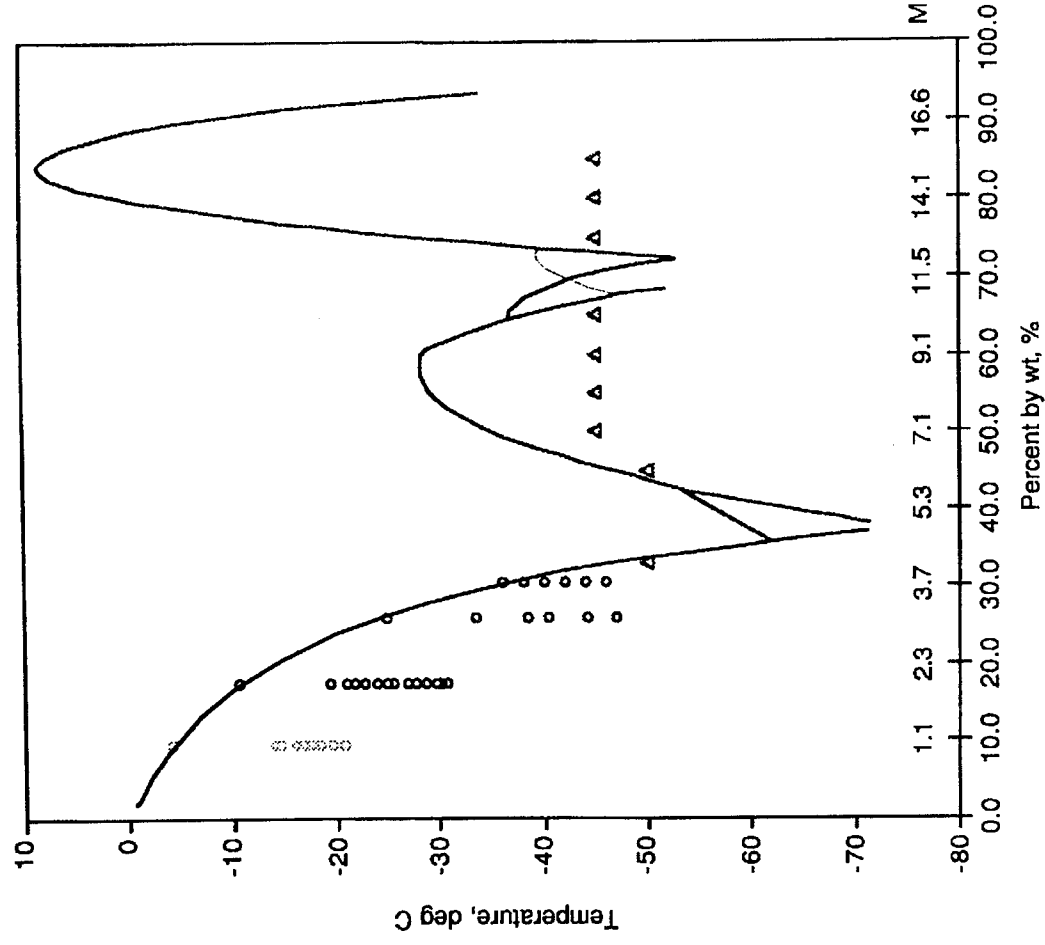
Figure 23. Equilibrium freezing temperatures and experimental data showing temperatures and molarity of nucleation. Triangles indicate points where nucleation was not initiated. (Gable, et al., 1950)

34
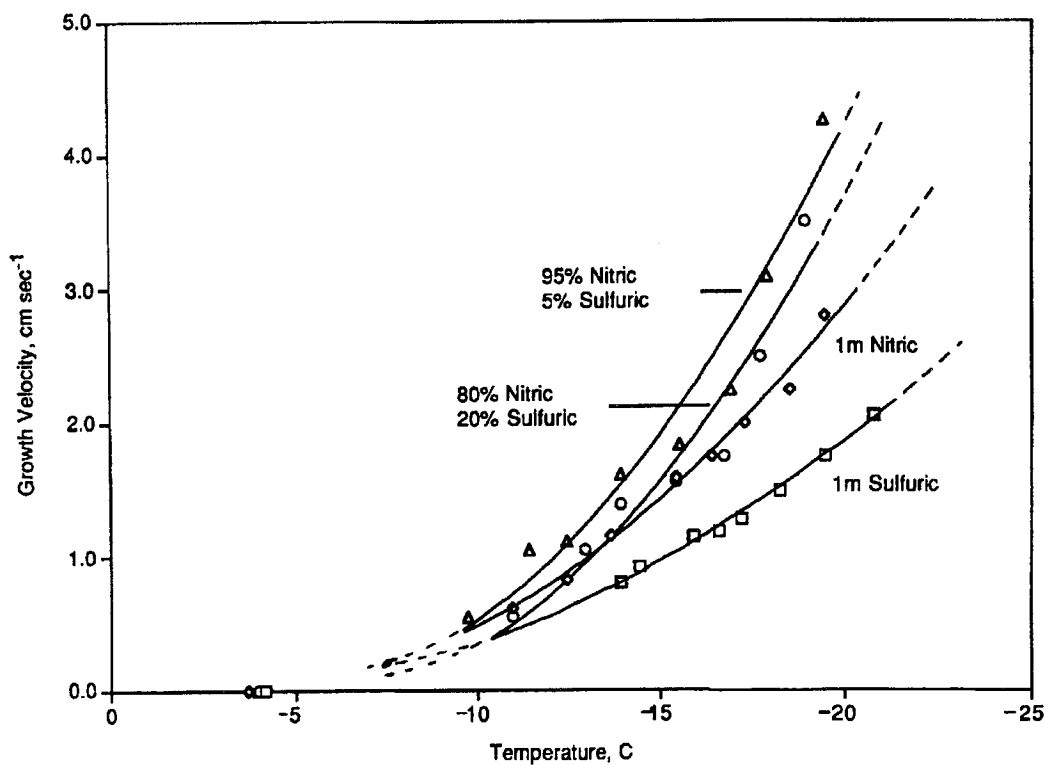
Figure 24. Growth velocity curves for 80% and 95% $HNO_3$ and 20% and 5% $H_2SO_4$ mixtures at 1 $m$.
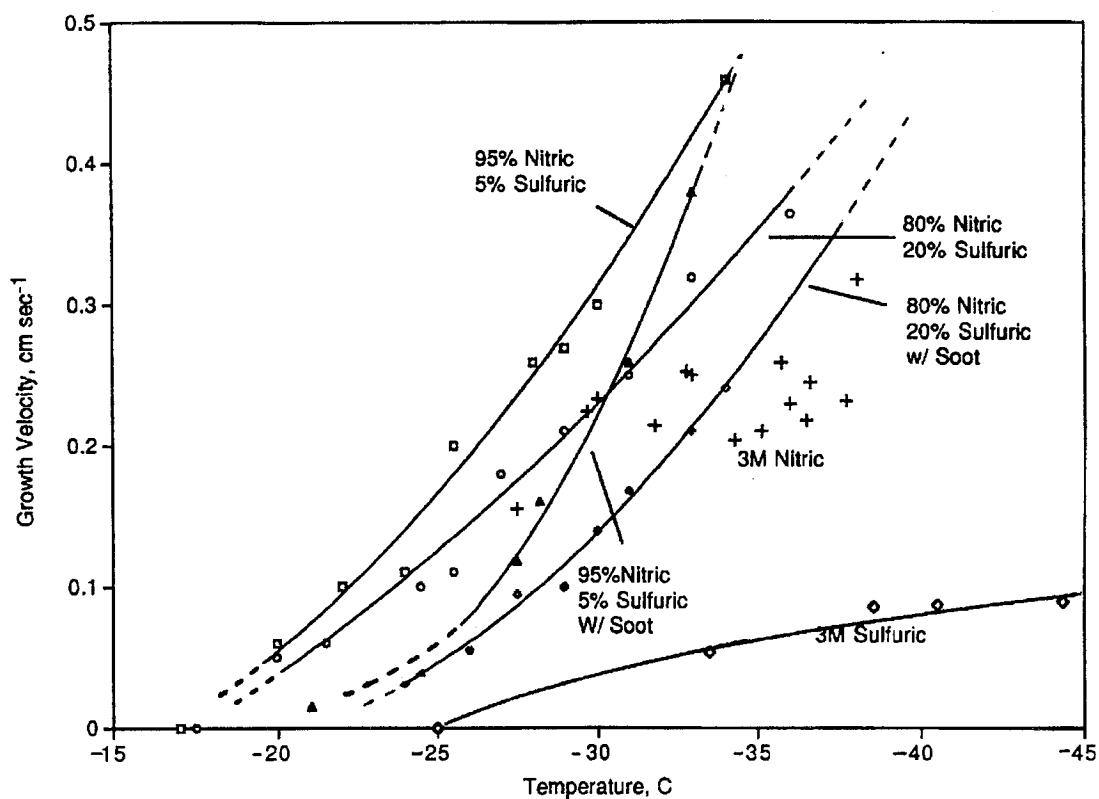


Figure 25. Growth velocity curves for 80% and 95% $HNO_3$ and 20% and 5% $H_2SO_4$ mixtures at 3 $m$. Curves also show the growth velocities for the same mixtures with a small amount of soot added.

## Addition of Non-Soluble Material

Soot is generally a non-soluble material and does not dissolve within a solution of sulfuric and nitric acid, but may affect the crystallization characteristics of the solution by acting as an impurity. As an impurity the soot should act to decrease the degree of supercooling and act to nucleate the solution earlier. Figure 24 shows the resulting curves for the addition of a small amount of soot into the 3.0 *M* mixtures. Indications by these growth curves seem to show a decrease in the growth rate for both mixtures. Also the data reveals that the addition of the soot has produced a few additional degrees of supercooling. If the soot were truly an active nucleating impurity, the nucleation point would actually be warmer. Hence the data from this experiment are suspect. As mentioned earlier, the exact age and composition of the soot is highly questionable. However, if the data are in fact valid, there must be some part of the soot particle that becomes part of the solution. The likelihood of aging processes or contaminants acquired postflight by the soot must be considered.

## CHAPTER 5: DISCUSSION OF RESULTS

Growth rates of solution are generally described by the equation $V = A(\Delta T)^P$ where $P$ is the best fit slope of the growth velocity on a log-log plot (figures 26 through 30). These plots show the slope for ammonium sulfate, ammonium bisulfate, sodium chloride, nitric acid, and sulfuric acid for each molality and molarity. The $P$ values for each are listed below:

| Ammonium Sulfate | Ammonium Bisulfate | Sodium Chloride |
|---|---|---|
| $P = 1.7 \pm 0.2$ (1 *m*) | $P = 1.88 \pm 0.2$ (1 *m*) | $P = 2.0 \pm 0.2$ (1 *m*) |
| $P = 1.5 \pm 0.2$ (2 *m*) | $P = 1.7 \pm 0.1$ (2 *m*) | $P = 2.0 \pm 0.2$ (2 *m*) |
| $P = 1.3 \pm 0.2$ (3 *m*) | $P = 1.3 \pm 0.1$ (3 *m*) | $P = 1.9 \pm 0.2$ (3 *m*) |
| $P = 0.99 \pm 0.1$ (4 *m*) | $P = 1.3 \pm 0.1$ (4 *m*) | $P = 1.7 \pm 0.2$ (4 *m*) |
| $P = 0.71 \pm 0.1$ (5 *m*) | $P = 1.1 \pm 0.2$ (5 *m*) | $P = 1.3 \pm 0.2$ (5 *m*) |
| $A = 0.015$ | $A = 0.02$ | $A = 0.022$ |

| Nitric Acid | Sulfuric Acid |
|---|---|
| $P = 1.9 \pm 0.2$ (2 *M*) | $P = 1.0 \pm 0.1$ (1 *M*) |
| $P = 0.55 \pm 0.1$ (2 *M*) | $P = 0.64 \pm 0.1$ (2 *M*) |
| $P = 0.44 \pm 0.1$ (3 *M*) | $P = 0.30 \pm 0.1$ (3 *M*) |
| | $P = 0.50 \pm 0.2$ (3.5 *M*) |
| $A = 0.011$ | $A = 0.007$ |

The values for $A$, are constant for a given substance; $V$ is in cm sec$^{-1}$.

These experimental results illustrate the point that ammonium sulfate, ammonium bisulfate, sodium chloride, and sulfuric and nitric acid, have complicated dependences of growth rate as compared to concentration. On these log-log plots it can be easily shown the approximate supercooling in which the viscosity effects begin to dominate. This is shown by the bending over of the curves to a slower growth rate. The experimental setup worked well over the course of this study, and has been shown to be very effective in obtaining growth velocities and supercooling data over the entire range of temperatures and concentrations.
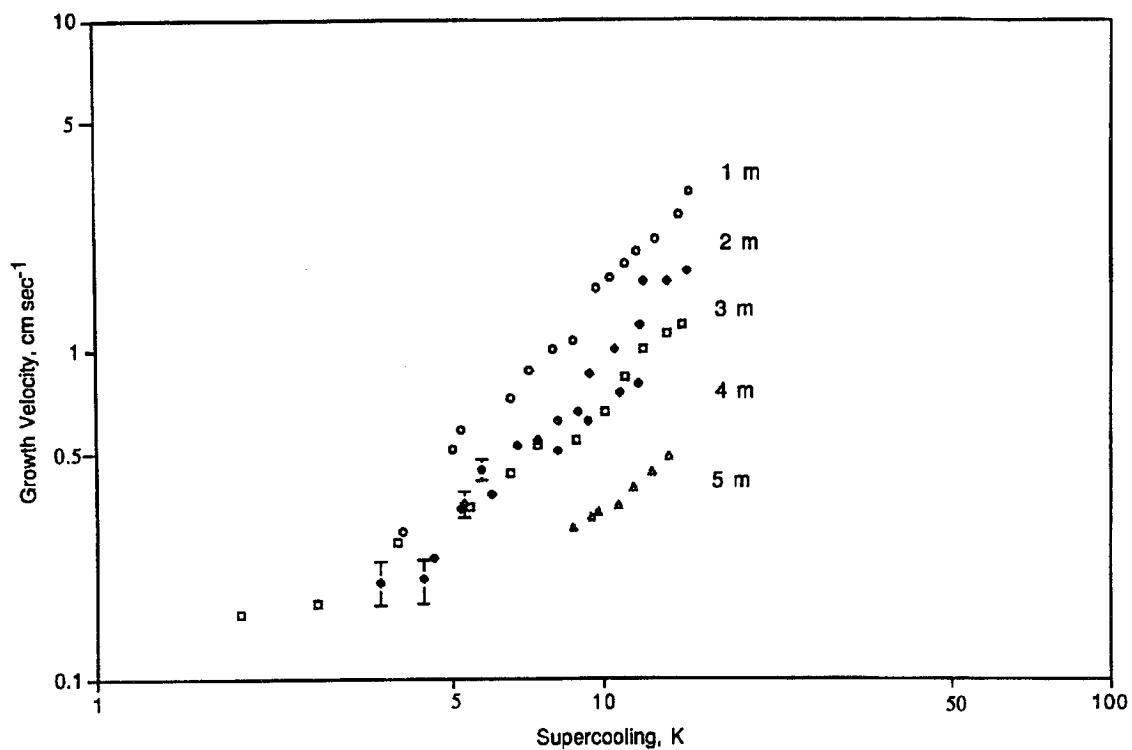
Figure 26. Growth velocity as a function of supercooling for sodium chloride.
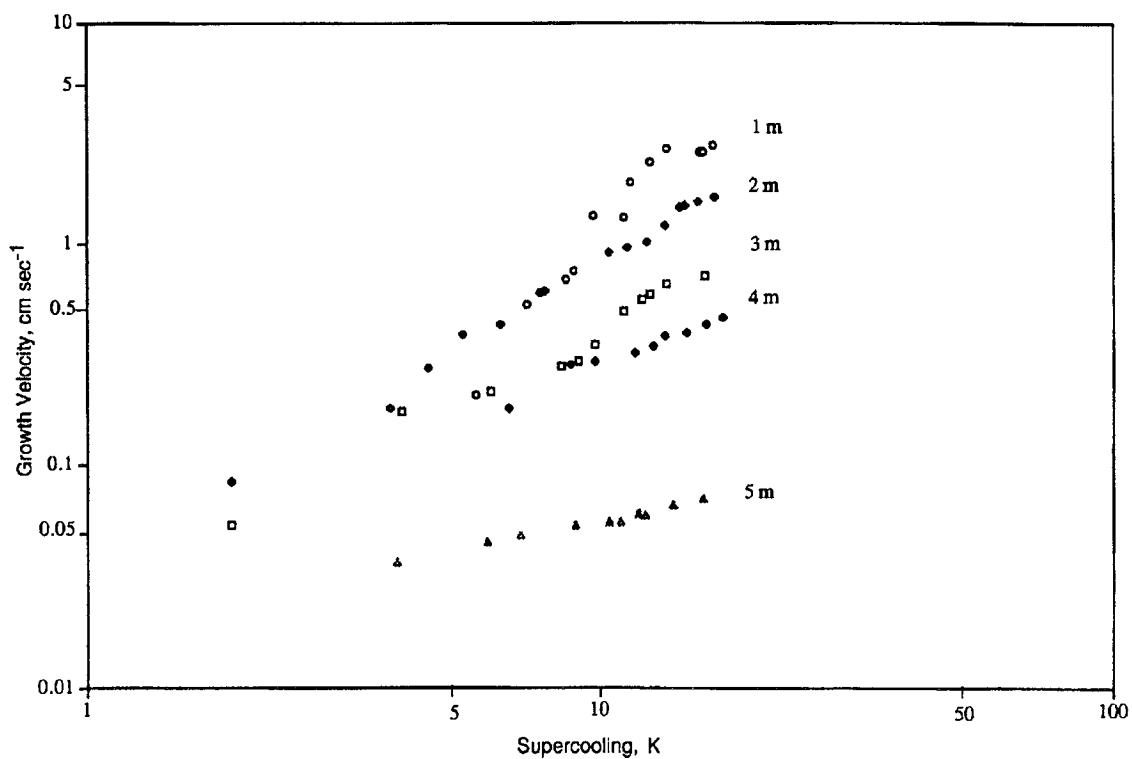


Figure 27. Growth velocity as a function of supercooling for ammonium bisulfate.
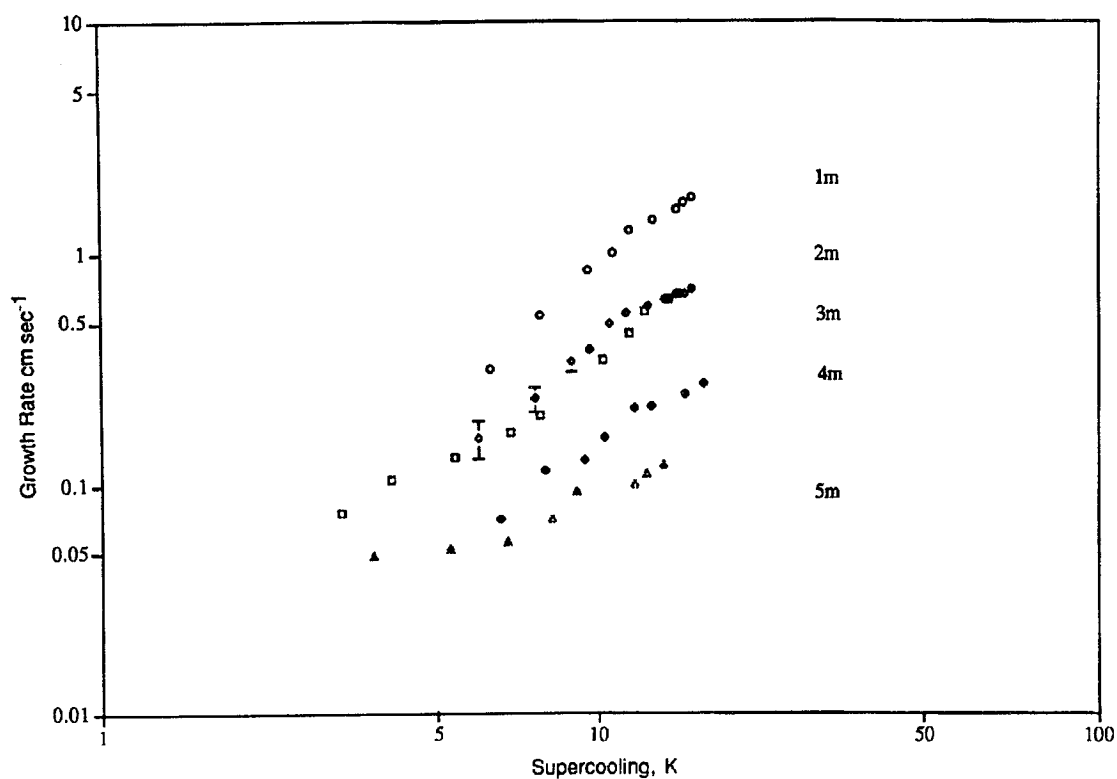
37

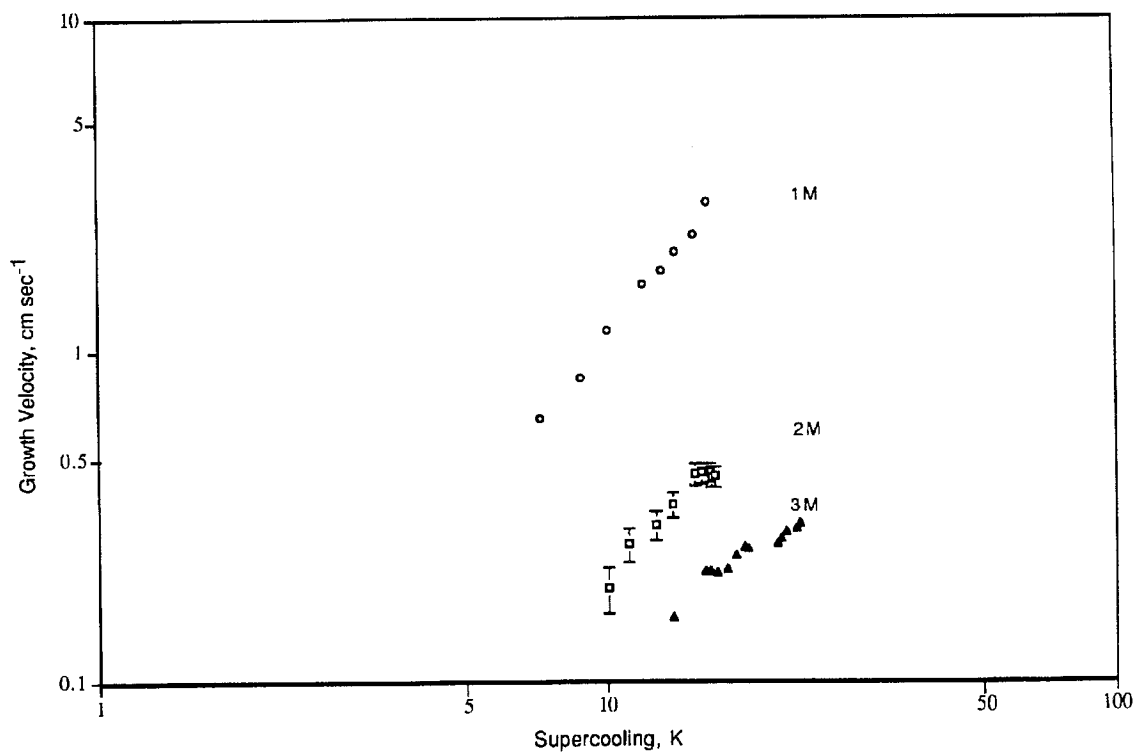Figure 28. Growth velocity as a function of supercooling for ammonium sulfate.



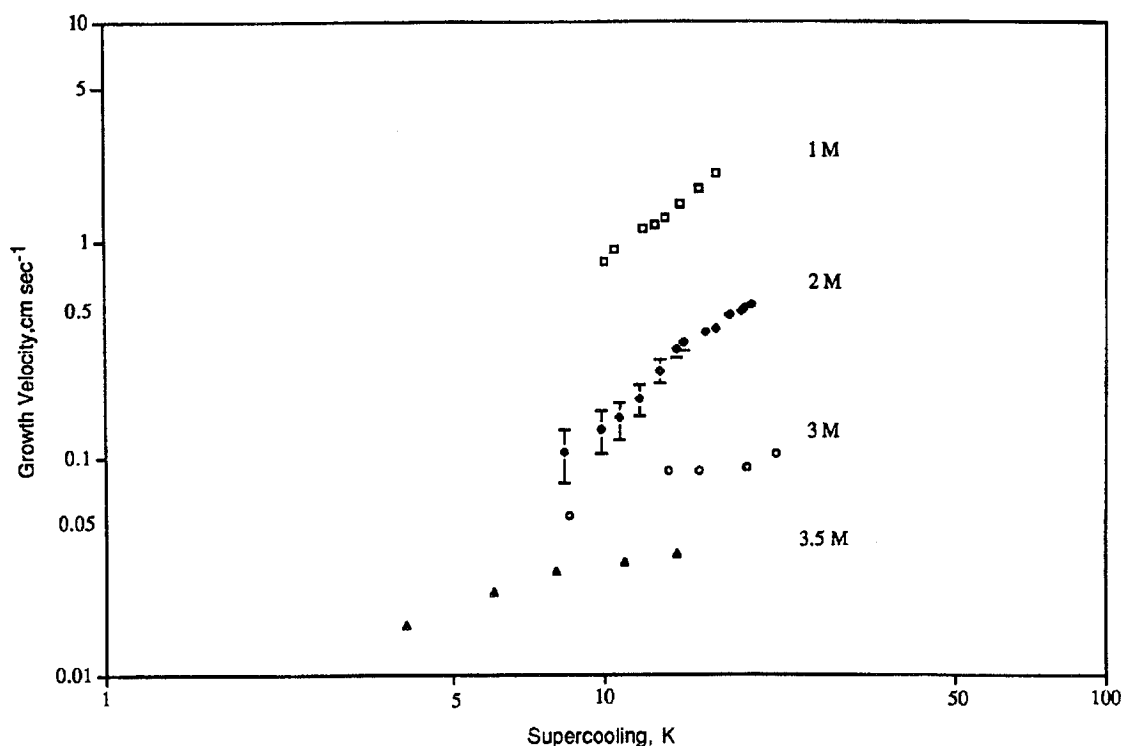Figure 29. Growth velocity as a function of supercooling for nitric acid.

Figure 30. Growth velocity as a function of supercooling for sulfuric acid.

The growth rates as a function of tube diameter show a strong dependence on tube diameter. The data show crystal growth rates within a glass tube are significantly reduced with decreasing diameter; conversely, the crystal growth rate increases with larger diameters. However, the data also show a limit in the crystallization rate with increasing diameter. In comparison, stratospheric cloud particles exist in relatively small volumes, on the order of about 4.0 $\mu m^3$, compared to the smallest volume used in this study of about 0.0412 $cm^3$ ($22/7 \times (0.025)^2 \times 21$ cm), or about 10 million times smaller. These results were similar to those found by Yang and Good (1966), who found that the size of the tubing directly affected the growth rate. The growth rates depend on the tube diameter, degree of supercooling, and the thermal conductivity of the tubing material. However, it is not clear which parameter controls the growth rates, and at what temperature the influence of these parameters change. A challenge exists to develop a system that will support the large supercooling of the smaller diameter tubing while allowing the growth rate of the larger diameters.

The growth rates for ammonium sulfate, ammonium bisulfate, and sodium chloride show that for a given concentration the growth rate increases with increasing supercooling, and at a given supercooling the growth rate decreases with increasing concentration. These results are consistent with those of O'Hare and Reed (1973). Indications from solubility tables (*International Critical Tables*, 1922) suggest that these materials may not contribute to the existence of the PSCs at normal stratospheric conditions, 1% relative humidity at 200 K. As illustrated by Twomey (1977), the phase transition of a particle from a solid to liquid will not occur until a sufficient relative humidity exists, shown in table 2. These conditions, in general, never exist. However, these materials are the natural material by which tropospheric processes such as fog and haze occur, with relative humidity significantly greater than the stratosphere.

The growth rate data suggest, as the concentrations increase, a tendency for the growth curves to reach a maximum followed by leveling off with supercooling. Consider the possibility that once this maximum rate is reached, and provided additional supercooling can be obtained, a decrease in growth rate can be observed, as

suggested by the alternate curve. If this actually occurs, and the volume is reduced sufficiently, it may be possible to achieve a point where no growth occurs, leaving the droplet in a so-called "glass transition." This glass transition has been characterized by a solution becoming so viscous due to the extreme supercooling, the droplet actually takes on glass-like characteristics. This glass, however, still a liquid, exhibits a high viscosity where the diffusion properties are reduced to those of a solid. In addition, the reduction of these properties may cause the heterogeneous reactions which once took place internally, to now occur only on the surface. However, because our test uses a sample volume many magnitudes larger than actual droplets it is difficult to determine whether a glass transition occurs with the volumes in this study. Appendices A and B show additional data describing the affects of temperature and viscosity on sulfuric and nitric acid respectively.

Sulfuric acid is very hygroscopic; it may not freeze at 100% by weight, and may never freeze as an aerosol due to viscosity effects. Figure 23 shows the assumed sulfuric acid equilibrium freezing temperature with respect to concentration, where at 38% by weight (7.5 $M$), a temperature of nearly $-80$ °C is required before nucleation can occur. This study was only able to nucleate sulfuric acid up to 3.5 $M$ (31% by weight). Ohtake's (1993) work illustrates similar problems. In his work he tried to nucleate sulfuric acid at all concentrations; however, at concentrations between 37.5% and 65% he was able to nucleate sulfuric acid at temperatures near $-65$ °C, but was not successful in attempts to nucleate sulfuric acid above concentrations of 65% by weight at temperatures of $-104$ °C. Ohtake discovered that the phase diagrams (represented in fig. 24) used from Gable, et al. (1950) were actually the melting points of sulfuric acid and its hydrates, instead of nucleation temperatures. Figure 6 shows how sulfuric acid deliquesces as a function of temperature in cases of a fixed mixing ratio.

For nitric acid the lowest equilibrium temperature was $-40$ °C, whereas sulfuric was $-80$ °C. Another characteristic that separated the two acids was viscosity as a function of concentration. At 100% by weight, sulfuric acid has a viscosity of 25.2 cP (Centipoise) at 20 °C, where nitric acid at 100% by weight has a viscosity less than water at 0.88 cP. For the higher concentrations, the nucleation temperatures were warmer, and nitric acid permitted nucleation. This became important when temperatures fell below 195 K. Figure 21(a) shows a change of growth rate because of temperature and viscosity changes. Significant growth rates are observed for equilibrium curves at temperatures between $-10$ to $-25$ °C. These curves show an increase in growth rate due to temperature. Also, when temperatures are below $-25$ °C the growth rates decrease due to viscosity effects. These conditions showed a growth rate increase of a factor of three, with a 2.0 $M$ increase in concentration and 10 °C warming. At the same temperature and a concentration increase of 1.0 $M$, for example, the viscosity increased and the growth rate decreased by one-third.

A phenomena was observed for nitric acid which demonstrates the presence of a hydrate. This consisted of a secondary crystallization. Initial crystal growth occurred in the normal observed way for 7.6 $M$ nitric acid at a temperature near $-50$ °C, 20 K supercooled at 0.2 cm sec$^{-1}$. The secondary growth occurred several minutes after the completion of the first, at a growth rate of about 0.01 cm sec$^{-1}$. This data was not illustrated on the figure presented. The second front had a whiter appearance, suggesting very fine crystals. This secondary front generally occurred at the higher concentrations, and could not be reliably repeated.

A significant increase in the growth rate is observed in a mixture of nitric and sulfuric acid for both the 1.0 $M$ and 3.0 $M$ concentrations. In addition, the data suggest that an increase in the equilibrium temperature freezing point may occur. Several runs were conducted showing good repeatability in the data. Molina, et al. (1993) have also shown that the growth rates will greatly increase with the addition of nitric acid into bulk sulfuric acid.

A limited number of runs were carried out in this study, with aircraft soot being added to the acid mixtures. The most important feature is the decrease of the nucleation temperature, which lowers the contribution from the mixture to nearly its original values. It is possible that in the atmosphere, the ternary $H_2SO_4 / H_2O / HNO_3$ exists and soot

40

mixes with a particle. If so, the aerosol may contain a small portion of unburned fuel that may contribute to an increased viscosity and concentration, thus reducing the crystal growth rate.

## Diffusion Chamber

Another method in analyzing the processes in PSC formation will involve the use of a thermal diffusion chamber. This study will combine processes to show the stages of PSC growth from aerosol activation to NAT crystal growth. This technique will be used to study the shape of the growing crystal under the influence of temperature, saturation ratio and supersaturation. This diffusion chamber will provide the controlled conditions necessary to aid in the simulated growth of the PSC, particularly the formation of the NAT particles. As a result of the experience with the present thermal diffusion chamber, recommendations for future test apparatus are described below. This recommended system will contain sulfate aerosols, water, and nitric acid vapor within two parallel plates separated by 3 cm. These two plates will each be temperature controlled by the use of thermoelectrics, and cooled by an external circulation bath system to withdraw heat produced by these thermoelectrics. Each plate will have a specified temperature with the top plate being warmer to provide the source of vapor, made of an acid resistant stainless steel, while the bottom plate will be colder to produce the supersaturation. The chamber walls will be made of acid resistant plastic. Temperature range will be from −90° C on the lower plate to −60 °C on the upper plate. A linear temperature gradient will establish a saturation vapor pressure curve (according to the Clausius-Clapeyron equation, as a function of temperature) between the lower and upper plates. This chamber can be adjusted to the desired temperature providing many degrees of supersaturations. However, since the nitric acid and water vapor each will have their own independent saturation profiles, there will exist two independent points of supersaturations between the plates. This point of maximum supersaturation will be the location where the crystals grow.

## Recommendations

In the future, improved testing techniques and equipment for temperatures to −100 °C should be considered a necessity in order to obtain the high degree of supercooling needed to validate the theory which describes the growth rate with decreasing temperatures. To complete the analysis of the supercooling effects, a design like the diffusion chamber would be useful to obtain the crystallization properties of the sulfuric-nitric acid mixtures, and to examine the true effects of supercooling and viscosity in a free environment on extremely small aerosol particles.

## Conclusions

Results from the present experiments indicate and support a theory that sulfuric acid aerosols may not be frozen at the temperatures where nitric acid uptake begins. This conclusion is obtained by the fact that $HNO_3$ uptakes onto aerosols at temperatures near 195 K. At that temperature, assuming normal stratospheric conditions, the droplet is about 50% $H_2SO_4$ by weight, and only 10 K supercooled. As shown in this study, sulfuric acid is not nucleated above 31% by weight (3.5 $M$). In addition, at temperatures below −50 °C, the viscosity effect is such that the probability of nucleation taking place becomes very low. However, this study has shown that if nitric acid can be added into the solution droplet, nucleation may be possible at higher temperatures.

The acid mixture data show a growth rate dependence on the $H_2SO_4$-$HNO_3$ mixture fraction and temperature. This implies that the probability of nucleation for a sulfuric acid particle increases with the presence of nitric acid. The adding of a non-reactive soot to a solution decreases the growth rate. Applying the volume theory, the droplet could become a glass at lower temperatures. To a small degree, the addition of soot to a solution tends to show a reduction in growth rate and supercooling. Whether this is considered important remains to be seen, but at a first glance may suggest some important factors regarding the formation of contrails, which are always observed with passing aircraft in cold atmospheric conditions.

In a realistic environment, sodium chloride, ammonium sulfate and ammonium bisulfate would not be considered a significant contribution to stratospheric aerosol. Since these salts would only be found as a solid aerosol, and their deliquescence point is too high, >70% RH, they could be neglected as a participant in PSC formation. However, these aerosols can be transported into the upper troposphere and lower stratosphere by deep convection, and depending upon the relative humidity reaching the deliquescence point, these particles may activate and become a high altitude haze or cirrus cloud. Figures 29 through 31 illustrate the change in equilibrium size with increasing humidity for ammonium sulfate, nitric acid, and sulfuric acid in Kohler curves. These Kohler curves also indicate the change in molality and molarity of each of the particles ranging in mass from $10^{-17}$ to $10^{-14}$ grams. Aerosols may also contribute to the production of visible contrails at high humidities. Cold temperatures, $<-60$ °C, during late fall and early spring, combined with the moisture advected by storm systems, may often provide these conditions.

## Implications

Increasing viscosity of high concentration solutions with decreasing temperature indicates a lowering of the diffusion coefficient. The diffusion coefficient for water is about $10^{-4}$; glass approaches $10^{-12}$ cm$^2$ sec$^{-1}$, comparable with a solid. The rate of diffusion of any size droplet is described by $r^2/D$. For a droplet of 1 μm, this means it takes $10^{-4}$ sec for water and $10^4$ sec for a glass. With lifetimes of some clouds being $10^3$ s, for PSC and cirrus, surface absorption reactions become important for ice and deeply supercooled stratospheric cloud particles; for liquid water droplets, the diffusion process occurs readily. It is not readily understood which process is the most important to each type of cloud.
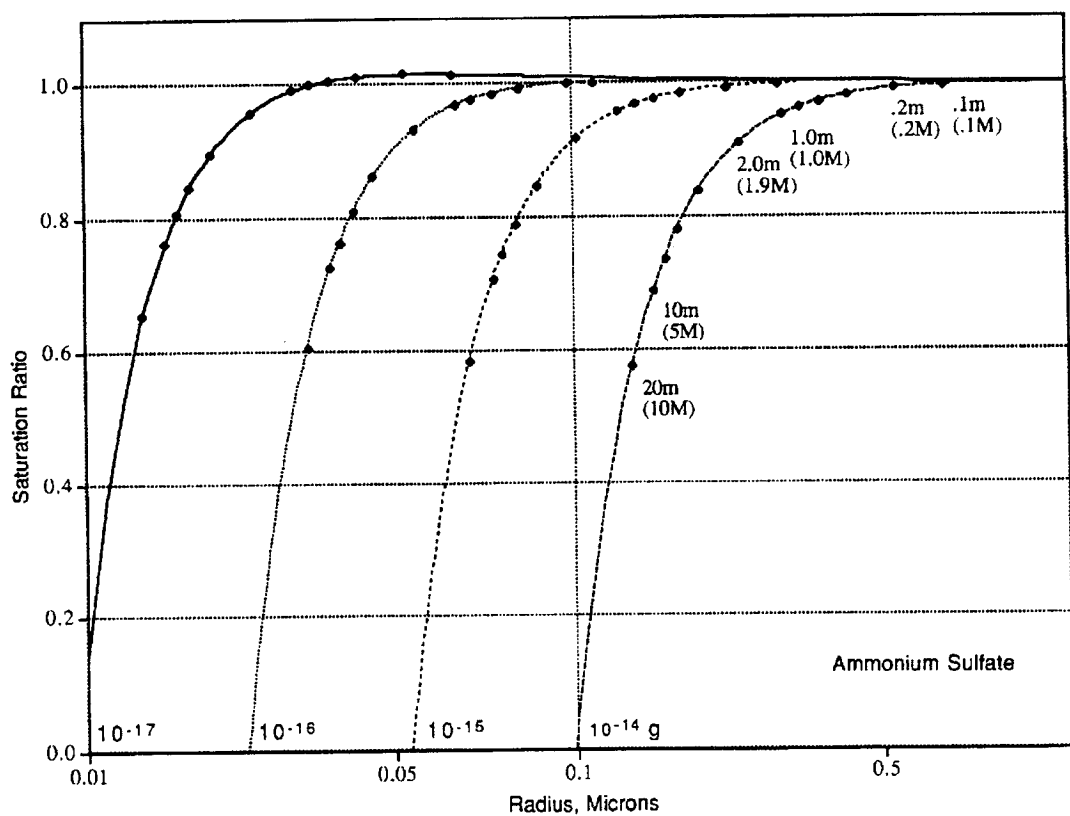


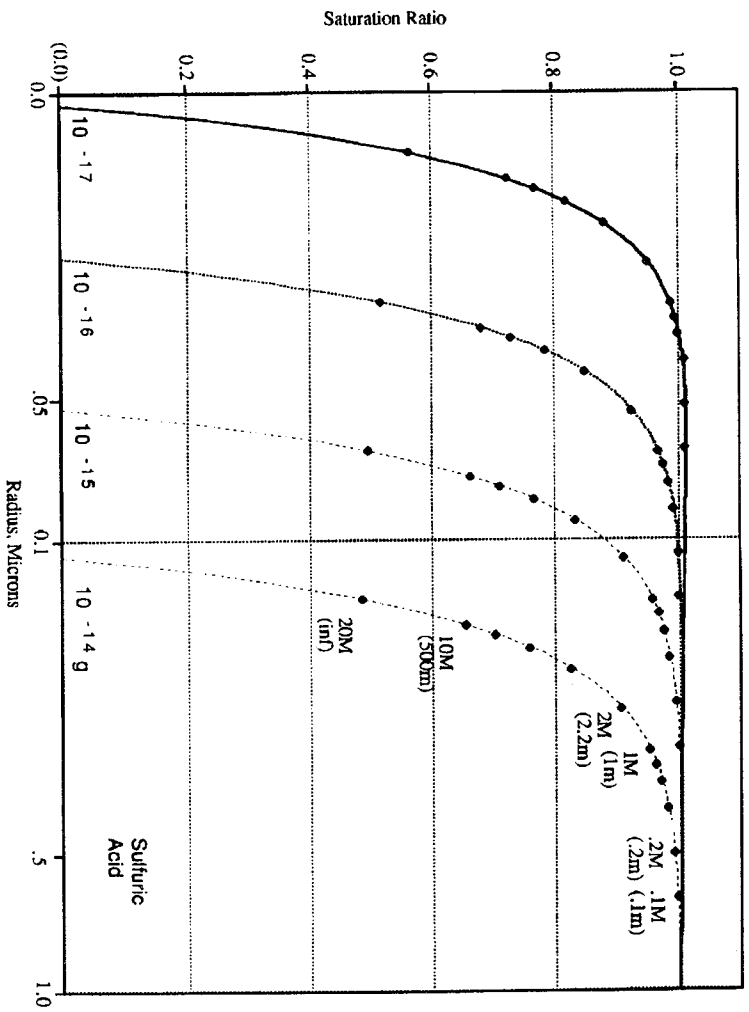(a) Ammonium sulfate.

Figure 31. Kohler curves for ammonium sulfate, nitric acid, sulfuric acid with molar and molal concentrations indicated.

42
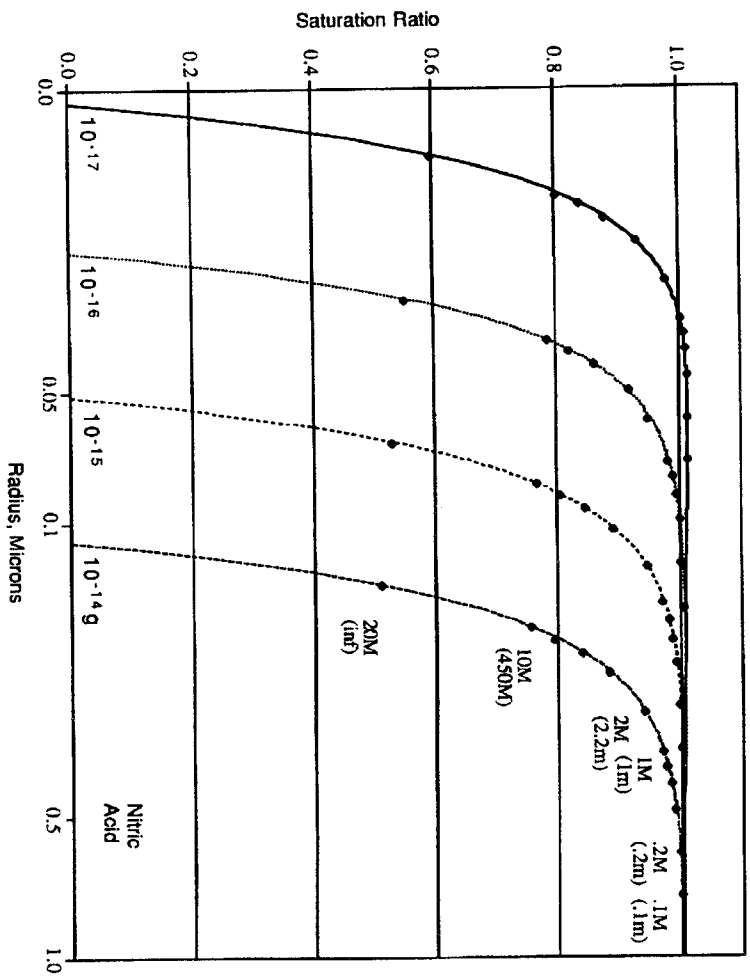
(c) Sulfuric acid.

(b). Nitric acid.

Figure 31. Kohler curves for ammonium sulfate, nitric acid, sulfuric acid with molar and molal concentrations indicated.

The addition of aircraft exhaust soot has been shown to hinder the growth and nucleation process of solutions. Why and how these effects occur need to be studied further and exhaust from a variety of aircraft must be used. It appears that depending on temperature and stratospheric water content, stratospheric cloud particles are able to exist in metastable compounds; however, these situations are extremely difficult to predict and should be viewed as the next research challenge.

The abundance of lower atmosphere aerosols may be useful as condensation cloud nuclei (CCN) for contrails. In addition to the natural aerosols present, the current aircraft fleet deposits a significant amount of particulate matter which produce contrails on a regular basis. There is some evidence, as observed by studying the sky sometime after a contrail has been produced, that on occasion the contrails will eventually form a cirrus cloud. However, because such material exists in the upper troposphere and lower stratosphere this matter should be considered by future investigations.

The overall implication is that particles at cirrus and PSC levels are capable of existing in a metastable condition. These particles may provide significant effects on chemical reaction rates through internal mixing, leading to ozone destruction; however, for highly viscous liquids only surface reactions occur.

# BIBLIOGRAPHY

Cadle, R. D., Grahek, F. E., Gandrud, B. W., and Lazrus, A. L., 1973: "Relative Efficiencies of Filters and Impactors for Collecting Stratospheric Particulate Matter," *J. Atmos. Sci.*, vol. 30, pp. 745–747.

Carslaw, H. S. and Jaeger, J. C., 1959: *Conduction of Heat in Solids,* 2nd ed., Clarendon Press.

Crutzen, Paul J. and Arnold, Frank, 1986: "Nitric Acid Cloud Formation in the Cold Arctic Stratosphere - A Major Cause for the Springtime 'Ozone Hole'," *Nature*, vol. 324, pp. 651–655.

Farman, J. C., Gardiner, B. G., and Shanklin, J. D., 1985: "Large Losses of Total Ozone in Antarctica Reveal Seasonal ClO(x)/NO(x) Interaction," *Nature*, vol. 315, pp. 207–210.

Friend, James P., Leifer, Robert, and Trichon, Morris, 1973: "On the Formation of Stratospheric Aerosols," *J. Atmos. Sci.*, vol. 30, pp. 465–479.

Gable, C. M., Batz, H. F., and Maron, S. H., 1950: "Phase Equilibria of the System Sulfur Trioxide-Water," *J. Amer. Chem. Soc.*, vol. 72, pp. 1445–1448.

Garcia, R. R. and Soloman, S., 1983: "A Numerical Model of the Zonally Averaged Dynamic and Chemical Structure of the Middle Atmosphere," *J. Geophys. Res.*, vol. 88, pp. 1379–1400.

Glasstone, Samuel and Lewis, David, 1960: *Elements of Physical Chemistry*, 2nd ed., Van Neustrian Co., Princeton, New Jersey.

Gmitro, John Irving and Vermeulen, Theodore, 1964: "Vapor-Liquid Equilibria for Aqueous Sulfuric Acid," *Amer. Inst. of Chem. Eng. J.*, vol. 10, no. 5, pp. 740–746.

Goodman, J., Toon, O. B., Pueschel, R. F., Snetsinger, K. G., and Verma, S., 1989: "Antarctic Stratospheric Ice Crystals," *J. Geophys. Res.*, vol. 94, pp. 16449–16457.

Hallett, J., 1964: "Experimental Studies of the Crystallization of Supercooled Water," *J. Atmos. Sci.*, vol. 21, pp. 671–682.

Hallett, J. and Lewis, R. E. J., 1967: "Mother-of-Pearl Clouds," *Weather*, vol. 22, no.2, pp. 56–65.

Hamill, P., Toon, O. B., and Kiang, C. S., 1977: "Microphysical Process Affecting Stratospheric Aerosol Particles," *J. Atmos. Sci.*, vol. 34, pp. 1104–1119.

Hamill, P., Turco, R. P., Kiang, C. S., Toon, O. B., and Whitten, R. C., 1982: "An Analysis of Various Nucleation Mechanism for Sulfate Particles in the Stratosphere," *J. Aerosol Sci.*, vol. 13, no. 6, pp. 561–585.

Hamill, P., McMaster, L. R., 1983: "Proceeding of a Workshop on Polar Stratospheric Clouds: Their Role in Atmospheric Processes," NASA-CP-2318.

Hamill, Patrick, Turco, R. P., and Toon, O. B., 1988: "On the Growth of Nitric and Sulfuric Acid Aerosol Particles Under Stratospheric Conditions," *J. Atmos. Chem*, vol. 7, pp. 287–315.

Hamill, Patrick and Toon, Owen B., 1991: "Polar Stratospheric Clouds and the Ozone Hole," *Physics Today*, vol. 44, pp. 34–42.

Hanson, David and Mauersberger, Konrad, 1988: "Laboratory Studies of the Nitric Acid Trihydrate - Implications for the South Polar Stratosphere," *Geophys. Res. Lett.*, vol. 15, pp. 855–858.

Hofmann, D. J., Rosen, J. M., Pepin, T. J., and Pinnick, R. G., 1975: "Stratospheric Aerosol Measurements. I - Time Variation at Northern Midlatitudes," *J. Atmos. Sci.*, vol. 32, pp. 1446–1456.

Hofmann, D. J., 1990: "Increase in the Stratospheric Background Sulfuric Acid Aerosol Mass in the Past 10 Years," *Science*, vol. 248, pp. 996–1000.

Humphreys-Owen, S. P. F., 1949: "Crystal Growth from Solution," *Proceedings of the Royal Society of London*, series A, vol. 197, no. A 1048, pp. 218–237.

Hunten, D. M., Turco, R. P., and Toon, O. B., 1980: "Smoke and Dust Particles of Meteoric Origin in the Mesosphere and Stratosphere," *J. Atmos. Sci.*, vol. 37, pp. 1342–1357.

*International Critical Tables of Numerical Data, Physics, Chemistry and Technology*, 1st ed., (1922), vol. 3, McGraw-Hill, New York.

Jet Propulsion Lab., <u>Chemical Kinetics and Photochemical Data for use in Stratospheric Modeling</u>, NASA-CR-176198, 1985. (Also published as JPL-PUB-85-37.)

Junge, Christian E, Chagnon, Charles W., and Manson, James E., 1961: "Stratospheric Aerosols," *J. Meteor.*, vol. 18, pp. 81–108.

Lindenmeyer, C. S, Orrok, G. T., Jackson, K. A., and Chalmers, B., 1957: "Rate of Growth of Ice Crystals in Supercooled Water," *J. Chem. Phys.*, vol. 27, no. 6, p. 822.

Low, Richard D. H., 1969: "A General Equation for the Solution Effect in Droplet Growth," *J. Atmos. Sci.*, vol. 26, pp. 608–611.

Mastenbrook, H. J., 1968: "Water Vapor Distribution in the Stratosphere and High Troposphere," *J. Atmos. Sci.*, vol. 25, pp. 299–311.

McCormick, M. P., Chu, W. P., Steele, H. M., Hamill, P., and Swissler, T. J., 1982: "Polar Stratospheric Cloud Sightings by SAM II—Stratospheric Aerosol Measurement Onboard Nimbus 7," *J. Atmos. Sci.*, vol. 39, pp. 1388–1397.

Molina, M. J., Zhang, R., Wooldridge, P. J., McMahon, J. R., Kim, J. E., Chang, H. Y., and Beyer, K. D., 1993: "Physical Chemistry of the $H_2SO_4/HNO_3/H_2O$ System: Implications for Polar Stratospheric Clouds," *Science*, vol. 261, pp. 1418–1423.

Nair, P. V. N. and Vohra, K. G., 1974: "Growth of Aqueous Sulfuric Acid Droplets as a Function of Relative Humidity," *J. Aerosol Sci.*, vol. 6, pp. 265–271.

Ohtake, Takeshi, 1993: "Freezing Points of $H_2SO_4$ Aqueous Solutions and Formation of Stratospheric Ice Clouds," *Tellus, Series B - Chemical and Physical Meteorology*, vol. 45B, no. 2, pp. 138-144.

O'Hare, M. and Reed, C. R., 1973: <u>Modeling Crystal Growth Rates From Solution</u>, Prentice-Hall, Inc., Englewood Cliffs, New Jersey, (out of print).

Pickering, S. U., 1893: "Isolation of Two Predicted Hydrates of Nitric acid," *J. Chem. Soc.*, vol. 63, pp. 436–443.

Poole, Lamont R. and McCormick, M. Patrick, 1988: "Polar Stratospheric Clouds and the Antarctic Ozone Hole," *J. Geophys. Res.*, vol. 93, pp. 8423–8430.

Pruppacher, H. R. and Neiburger, M., 1963: "The Effects of Water Soluble Substances on the Supercooling of Water Droplets," *J. Atmos. Sci., vol.* 20, pp. 376–385.

Pueschel, R. F., Ferry, G. V., Snetsinger, K. G., Goodman, J., Dye, J. E., Baumgardner, D., and Gandrud, B. W., 1992: "A Case of Type I Polar Stratospheric Cloud Formation by Heterogeneous Nucleation," *J. Geophys. Res.*, vol. 97, no.D8, pp. 8105–8114.

Rosen, James M, 1964: "The Vertical Distribution of Dust to 30 Kilometers," *J. Geophys. Res.*, vol. 69, no. 21, pp. 4673–4676.

Rosen, J. M., Hofmann, D. J., and Laby, J., 1975: "Stratospheric Aerosol Measurements. II - The Worldwide Distribution," *J. Atmos. Sci.*, vol. 32, pp. 1457–1462.

Salawitch, R. J., Gobbi, G. P., Wofsy, S. C., and McElroy, M. B., 1989: "Denitrofication in the Antarctic Stratosphere," *Nature*, vol. 339, pp. 525–527.

Steele, Helen M., and Hamill, Patrick, 1981: "Effects of Temperature and Humidity on the Growth and Optical Properties of Sulfuric Acid-Water Droplets in the Stratosphere," *J. Aerosol. Sci.*, vol. 12, no. 6, pp. 517–528.

Steele, H. M., Hamill, P., Swissler, T. J., and McCormick, M. P., 1983: "The Formation of Polar Stratospheric Clouds," *J. Atmos. Sci.*, vol. 40, pp. 2055–2067.

Toon, Owen B., Pinto, Joseph, Hamill, Patrick, and Turco, Richard P., 1986: "Condensation of $HNO_3$ and HCl in the Winter Polar Stratospheres," *Geophys. Res. Lett.*, vol. 13, pp. 1284–1287.

Toon, Owen B., Ferry, G., Turco, R. P., Jordan, J., and Goodman, J., 1989: "Physical Processes in Polar Stratospheric Ice Clouds," *J. Geophys. Res.*, vol. 94, pp. 11359–11380.

Turco, Richard P., Toon, Owen B., and Hamill, Patrick, 1989: "Heterogeneous Physicochemistry of the Polar Ozone Hole," *J. Geophys. Res.*, vol. 94, pp. 16493–16510.

Twomey, S., 1977: Atmospheric Aerosols, Series 7, Elsevier Scientific Publishing Co., New York.

U. S. Standard Atmosphere, 1976, U. S. Government Printing Office, Washington, D.C.

Yang, L. C. and Good, W. B., 1966: "Crystallization Rate of Supercooled Water in Cylindrical Tubes," *J. Geophys. Res.*, vol. 71, no.10, pp. 2465–2469.

Wedum, Ellen Elisabeth, 1979: "Schlieren Studies of Crystallization in Supercooled Sodium Sulfate Solution," M. S. Thesis, University of Nevada, Reno.

# APPENDIX A: CHEMICAL REACTIONS WHICH PRODUCE SULFURIC ACID

According to laboratory experiments conducted by Friend, et al. (1973), the proposed stratospheric chemical reactions that lead to stratospheric sulfate aerosols are:
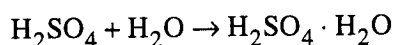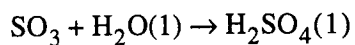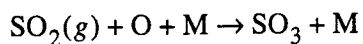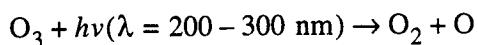
$$O_3 + h\nu(\lambda = 200 - 300 \text{ nm}) \rightarrow O_2 + O$$

$$SO_2(g) + O + M \rightarrow SO_3 + M$$

$$SO_3 + H_2O(l) \rightarrow H_2SO_4(l)$$

$$H_2SO_4 + H_2O \rightarrow H_2SO_4 \cdot H_2O$$

Table A-1. Vapor pressures (mm Hg) $H_2SO_4$ and $H_2O$ in solution. (Gmitro and Vermeulen, 1964).

| Temperature, (K) | | Weight percent $H_2SO_4$ | | | | | |
|---|---|---|---|---|---|---|---|
| | | 70 | 72 | 74 | 76 | 78 | 80 |
| 218.16 | $H_2SO_4$ | $1.3 \times E{-}14$ | $3.58 \times E{-}14$ | $1.0 \times E{-}13$ | $2.86 \times E{-}13$ | $8.25 \times E{-}13$ | $2.52 \times E{-}12$ |
| | $H_2O$ | $4.17 \times E{-}4$ | $2.68 \times E{-}3$ | $1.6 \times E{-}3$ | $8.97 \times E{-}5$ | $4.97 \times E{-}5$ | $2.18 \times E{-}5$ |
| 223.16 | $H_2SO_4$ | $5.02 \times E{-}14$ | $1.35 \times E{-}13$ | $3.7 \times E{-}13$ | $1.03 \times E{-}12$ | $2.93 \times E{-}12$ | $8.69 \times E{-}12$ |
| | $H_2O$ | $8.16 \times E{-}4$ | $5.23 \times E{-}4$ | $3.17 \times E{-}4$ | $1.8 \times E{-}4$ | $9.46 \times E{-}5$ | $4.49 \times E{-}5$ |
| 228.16 | $H_2SO_4$ | $1.81 \times E{-}13$ | $4.7 \times E{-}13$ | $1.29 \times E{-}12$ | $3.51 \times E{-}12$ | $9.78 \times E{-}12$ | $2.82 \times E{-}11$ |
| | $H_2O$ | $1.54 \times E{-}3$ | $9.93 \times E{-}4$ | $6.08 \times E{-}4$ | $3.5 \times E{-}4$ | $1.86 \times E{-}4$ | $8.99 \times E{-}5$ |
| 233.16 | $H_2SO_4$ | $6.17 \times E{-}13$ | $1.51 \times E{-}12$ | $4.23 \times E{-}12$ | $1.13 \times E{-}11$ | $3.08 \times E{-}11$ | $8.67 \times E{-}11$ |
| | $H_2O$ | $2.82 \times E{-}3$ | $1.83 \times E{-}3$ | $1.13 \times E{-}3$ | $6.58 \times E{-}4$ | $3.55 \times E{-}4$ | $1.75 \times E{-}4$ |
| 238.16 | $H_2SO_4$ | $1.99 \times E{-}12$ | $5.12 \times E{-}12$ | $1.32 \times E{-}11$ | $3.47 \times E{-}11$ | $9.24 \times E{-}11$ | $2.43 \times E{-}10$ |
| | $H_2O$ | $5.03 \times E{-}3$ | $3.23 \times E{-}3$ | $2.06 \times E{-}3$ | $1.21 \times E{-}3$ | $6.6 \times E{-}4$ | $3.3 \times E{-}4$ |

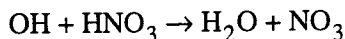# APPENDIX B: PHOTOCHEMICAL REACTIONS
# LEADING TO NITRIC ACID FORMATION

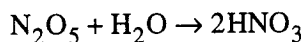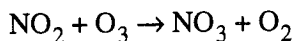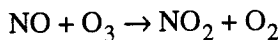Jet Propulsion Laboratory (1985) suggests that nitric acid is produced by the following reactions

$$OH + NO_2 + M \rightarrow HNO_3 + M$$
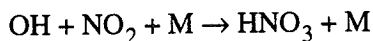
and destroyed by photolysis

$$HNO_3 + h\nu(\lambda = 320 \text{ nm}) \rightarrow OH + NO_2$$
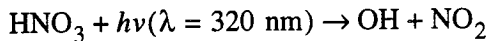
and reactions with OH

$$OH + HNO_3 \rightarrow H_2O + NO_3$$
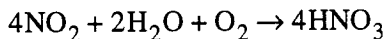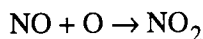
There are, in addition to these, many more reactions that lead to the formation and subsequent buildup of $HNO_3$;

$$NO + O_3 \rightarrow NO_2 + O_2$$

$$NO_2 + O_3 \rightarrow NO_3 + O_2$$

$$NO_2 + NO_3 + M \rightarrow N_2O_5 + M$$

$$N_2O_5 + H_2O \rightarrow 2HNO_3$$

Another possible formation reaction of $HNO_3$ in the absence of $N_2O_5$ is

$$NO + O \rightarrow NO_2$$

$$4NO_2 + 2H_2O + O_2 \rightarrow 4HNO_3$$

Since the duration of sunlight during the winter months is a function of latitude, the lifetimes of $HNO_3$ can vary throughout the stratosphere and can be shown to be dependent on latitude. After nitric acid has formed it can then aid in growth of PSCs under particular stratospheric conditions by condensation onto frozen sulfate aerosols or other existing aerosols when temperatures fall below 200 K.
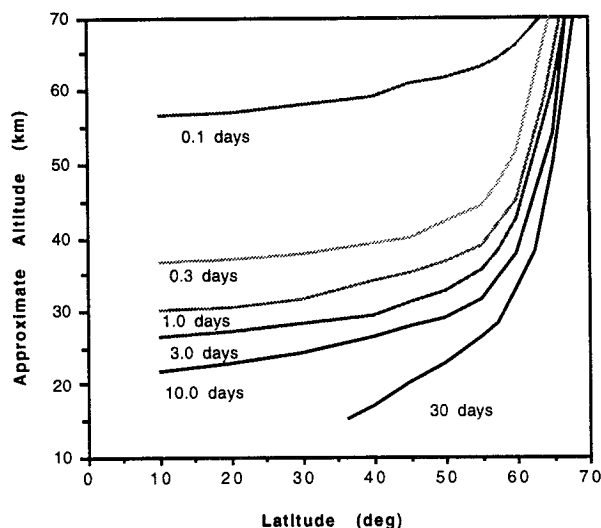


Figure B-1. Photochemical lifetime of $HNO_3$ for winter, as calculated by Garcia-Soloman (1983) as a function of altitude and latitude.

# APPENDIX C

Table C-1. Thermal properties of common substances. (Carslaw and Jaeger, 1959)

| Substance | Density, $g\ cm^{-3}$ | Specific heat, $cal\ g^{-1}\ K^{-1}$ | Conductivity, $cal\ cm^{-1}\ sec^{-1}\ K^{-1}$ | Diffusivity, $cm^2\ sec^{-1}$ |
|---|---|---|---|---|
| Copper | 10.49 | 0.0556 | 1.00 | 1.14 |
| Silver | 9.94 | 0.93 | 0.93 | 1.71 |
| Brass | 8.5 | 0.09 | 0.25 | 0.33 |
| Steel | 7.85 | 0.118 | 0.11 | 0.12 |
| Air | 0.00129 | 0.24 | 0.000058 | 0.187 |
| Ice | 0.92 | 0.502 | 0.0053 | 0.0115 |
| Glass | 2.4 | 0.20 | 0.0028 | 0.0058 |
| Snow | 0.1 | 0.5 | 0.00025 | 0.005 |
| Water | 1.0 | 1.0 | 0.00144 | 0.00144 |

| REPORT DOCUMENTATION PAGE | Form Approved OMB No. 0704-0188 |
|---|---|

Public reporting burden for this collection of information is estimated to average 1 hour per response, including the time for reviewing instructions, searching existing data sources, gathering and maintaining the data needed, and completing and reviewing the collection of information. Send comments regarding this burden estimate or any other aspect of this collection of information, including suggestions for reducing this burden, to Washington Headquarters Services, Directorate for Information Operations and Reports, 1215 Jefferson Davis Highway, Suite 1204, Arlington, VA 22202-4302, and to the Office of Management and Budget, Paperwork Reduction Project (0704-0188), Washington, DC 20503.

| 1. AGENCY USE ONLY (Leave blank) | 2. REPORT DATE<br>March 1997 | 3. REPORT TYPE AND DATES COVERED<br>Contractor Report | |
|---|---|---|---|

**4. TITLE AND SUBTITLE**

A Laboratory Study on the Phase Transition for Polar Stratospheric Cloud Particles

**5. FUNDING NUMBERS**

WU 529-10-04

**6. AUTHOR(S)**

Edward H. Teets, Jr.

**7. PERFORMING ORGANIZATION NAME(S) AND ADDRESS(ES)**

NASA Dryden Flight Research Center
P.O. Box 273
Edwards, California 93523-0273

**8. PERFORMING ORGANIZATION REPORT NUMBER**

H-2147

**9. SPONSORING/MONITORING AGENCY NAME(S) AND ADDRESS(ES)**

National Aeronautics and Space Administration
Washington, DC 20546-0001

**10. SPONSORING/MONITORING AGENCY REPORT NUMBER**

NASA CR-198056
NASA Contract NAG-2572

**11. SUPPLEMENTARY NOTES**

**12a. DISTRIBUTION/AVAILABILITY STATEMENT**

Unclassified—Unlimited
Subject Category 46

**12b. DISTRIBUTION CODE**

**13. ABSTRACT (Maximum 200 words)**

The nucleation and growth of different phases of simulated polar stratospheric cloud (PSC) particles were investigated in the laboratory. Solutions and mixtures of solutions at concentrations 1 to 5 $m$ (molality) of ammonium sulfate, ammonium bisulfate, sodium chloride, sulfuric acid, and nitric acid were supercooled to prescribed temperatures below their equilibrium melting point. These solutions were contained in small diameter glass tubing of volumes ranging from 2.6 to 0.04 ml. Samples were nucleated by insertion of an ice crystal, or in some cases by a liquid nitrogen cooled wire. Crystallization velocities were determined by timing the crystal growth front passages along the glass tubing. Solution mixtures containing aircraft exhaust (soot) were also examined. Crystallization rates increased as $\Delta T^2$, where $\Delta T$ is the supercooling for weak solutions (2 $m$ or less). The higher concentrated solutions ($>3$ $m$) showed rates significantly less than $\Delta T^2$. This reduced rate suggested an onset of a glass phase. Results were applied to the nucleation of highly concentrated solutions at various stages of polar stratospheric cloud development within the polar stratosphere.

**14. SUBJECT TERMS**

Cloud research, Crystals, Stratospheric circulation, Temperature effects, Thermodynamic properties of liquids

**15. NUMBER OF PAGES**
58

**16. PRICE CODE**
A04

| 17. SECURITY CLASSIFICATION OF REPORT<br>Unclassified | 18. SECURITY CLASSIFICATION OF THIS PAGE<br>Unclassified | 19. SECURITY CLASSIFICATION OF ABSTRACT<br>Unclassified | 20. LIMITATION OF ABSTRACT<br>Unlimited |
|---|---|---|---|

NSN 7540-01-280-5500      Available from the NASA Center for AeroSpace Information, 800 Elkridge Landing Road, Linthicum Heights, MD 21090; (301)621-0390

Standard Form 298 (Rev. 2-89)
Prescribed by ANSI Std. Z39-18
298-102

National Aeronautics and
Space Administration
Code JTT
Washington, D.C. 20546-0001
USA

POSTMASTER: If Undeliverable (Section 158
Postal manual) Do Not Return